Tackling the conformational sampling of larger flexible compounds and macrocycles in pharmacology and drug discovery

I-Jen Chen *, Nicolas Foloppe *

Vernalis (R&D) Ltd, Granta Park, Abington, Cambridge CB21 6GB, UK

ABSTRACT

Computational conformational sampling underpins much of molecular modeling and design in pharmaceutical work. The sampling of smaller drug-like compounds has been an active area of research. However, few studies have tested in details the sampling of larger more flexible compounds, which are also relevant to drug discovery, including therapeutic peptides, macrocycles, and inhibitors of protein–protein interactions. Here, we investigate extensively mainstream conformational sampling methods on three carefully curated compound sets, namely the 'Drug-like', larger 'Flexible', and 'Macrocycle' compounds. These test molecules are chemically diverse with reliable X-ray protein-bound bioactive structures. The compared sampling methods include Stochastic Search and the recent LowModeMD from MOE, all the low-mode based approaches from MacroModel, and MD/LLMOD recently developed for macrocycles. In addition to default settings, key parameters of the sampling protocols were explored. The performance of the computational protocols was assessed via (i) the reproduction of the X-ray bioactive structures, (ii) the size, coverage and diversity of the output conformational ensembles, (iii) the compactness/extendedness of the conformers, and (iv) the ability to locate the global energy minimum. The influence of the stochastic nature of the searches on the results was also examined. Much better results were obtained by adopting search parameters enhanced over the default settings, while maintaining computational tractability. In MOE, the recent LowModeMD emerged as the method of choice. Mixed torsional/low-mode from MacroModel performed as well as LowModeMD, and MD/LLMOD performed well for macrocycles. The low-mode based approaches yielded very encouraging results with the flexible and macrocycle sets. Thus, one can productively tackle the computational conformational search of larger flexible compounds for drug discovery, including macrocycles.

© 2013 Elsevier Ltd. All rights reserved.

1. Introduction

Conformational sampling underpins much of the computational modeling of the three-dimensional (3D) conformations and properties of organic compounds. In medicinal chemistry and pharmacology, the compound conformations are a critical input for many analyses and molecular design efforts, regarding conformational analysis,[1–3] examination of intramolecular contacts,[4] the effect of conformation on reactivity,[5] the influence of crystal lattices on conformations,[6] fitting of molecular models to the X-ray electron density maps,[7,8] interpretation of NMR data,[9–12] compound overlays,[13,14] pharmacophore elucidation,[15] pharmacophore-based[16] and shape-based[17] virtual screening, docking to a receptor,[18] exploitation of molecular fields,[19] and estimates of the conformational energy of bound ligands.[20–23] These tasks require an ensemble of conformations for every compound, since flexible compounds interconvert between low-energy conformations. Therefore, the conformational sampling of small molecules is a very active area of research.[22,24–39]

To generate conformers, computational methods rely on an energy model and a sampling algorithm which acts on the conformational degrees of freedom. The many methods devised to sample the conformational space and the underlying energy models have been reviewed.[38,39] Search methods typically involve a stochastic element, which may be torsional Monte Carlo moves,[40] random pulses in Cartesian coordinates,[41] seed inter-atomic distances in distance geometry calculations,[24] initial velocities of a molecular dynamics simulation,[42] or the chosen low-modes and seed conformer in low-mode searches.[34,43] Thanks to improved computational resources, algorithmic innovations,[9,34,44,45] and optimization of the search parameters that control a sampling protocol,[30] the conformational sampling of relatively small drug-like compounds with only moderate flexibility has become very powerful.[46]

Thus, it is timely to address the conformational sampling of compounds larger and more flexible than conventionally smaller 'drug-like' compounds. Indeed, a good number of approved drugs are larger and more flexible than required by mainstream drug-likeness criteria;[24,27,47] examples include lipitor, eribulin,[48] and a number of antibiotics.[49] In addition, there is a resurgence of interest in chemotypes which do not fit narrow drug-like prescriptions, such as therapeutic peptides[50] and macrocycles.[27,34,51] Inhibitors of protein–protein interactions also tend to be larger and more flexible since, to gain binding affinity for rather flat and open binding sites, they have to make numerous contacts with the protein.[52] In addition, pharmacology is not only concerned with drug candidates, but also with tool compounds which can be quite flexible. Also, modelling of larger compounds may reveal a key binding fragment core, from which new smaller and more ligand-efficient compounds could be designed. Therefore, conformational sampling of large flexible compounds is of general interest.

Indeed, recent studies have started to investigate the conformational sampling of more flexible compounds, for example with Monte-Carlo torsional sampling,[53] distance geometry[24,27] and the LowModeMD method which combines low-mode and MD sampling.[34] Distance geometry is an interesting approach since it can incorporate heuristics which bias the search towards more extended or more compact conformers, to direct the search across a range of molecular compactness values.[24] It can handle macrocycles.[27] Low-mode based methods are also of special interest for flexible and/or cyclic compounds.[9,34,43,54,55] The principle of low-mode search methods has been explained.[9] Briefly, the low-frequency vibrational mode eigenvectors can be seen as pointing along the low-energy paths connecting energy minima via saddle points on the conformational energy surface. So, moving the coordinates along the low-frequency modes is an efficient way to cross energy barriers between energy minima; once a move following a low-mode eigenvector has located a new energy well, energy minimization is performed and another search cycle is initiated. It has the advantage to be performed in the space of reduced dimensionality of the low-frequency modes, and is well-adapted to cyclic topologies. Low-mode searches can be tuned by controlling how frequently the eigenvectors are re-calculated along the search. To apply low-mode based searches to large systems, at least two approaches have been devised, the Large-scale low mode method (LLMOD),[43] and the recently developed LowModeMD approach[34] implemented in the software MOE.[56] LLMOD generates the eigenvectors without explicitly diagonalizing the entire Hessian.[43] LowModeMD does not calculate the low-frequency modes explicitly, but instead efficiently channels and amplifies atomic motions along directions of low curvature of the potential energy surface,[34] that is along directions similar to those followed by the low-frequency modes. The vibrational motions are imparted via a short molecular dynamics (MD) run at the beginning of every iteration. Initial tests of LowModeMD with macrocycles and protein loops have been encouraging,[34] but it is important to assess further the

performance of this new method. Moreover, various low-mode based search schemes have long been implemented in the widely used MacroModel package[57] distributed by Schrödinger.[58] MacroModel offers a plain low-mode search termed Low-mode (LMOD), and the variant Large-scale low-mode (LLMOD) which obtains the eigenvectors in a more approximate manner that is more efficient for larger systems.[43] Two other variants add random torsional moves to the low-mode sampling, and are called Mixed torsional/Low-mode (MT/LMOD) and Mixed torsional/Large-scale low-mode (MT/LLMOD). Schrödinger has also recently proposed a specialized method to explore the conformational space of macrocycles, which starts with a high-temperature MD-based simulated annealing followed by LLMOD sampling; we refer to this method as MD/LLMOD. Thus, low-mode based sampling methods are conceptually well-adapted to the conformational sampling of larger flexible compounds, and are widely available from mainstream software. Also, it is of interest to assess if the recent developments implemented in LowModeMD[34] offer advantages over the earlier incarnations of low-mode based searches,[9,43,54] or over the MOE Stochastic Search.

Low-mode search approaches have been investiagted,[9,24,27,33,34,43,54,59,60] but early studies usually could only handle a small number of compounds, and most studies were essentially performed at the default settings of the program. Yet, conformational sampling protocols depend on many tunable settings which can be adjusted and strongly influence their performance. Such settings include the number of search cycles, the energy window within which the conformers are accepted, how similar to each other the retained conformers can be, and variants on the energy model. Consequently, a more systematic assessment of low-mode search methods would provide guidance regarding best-practices for medicinal chemistry applications and data to compare search algorithms, while clarifying what can be expected of these methods for particularly flexible compounds. Such results may give hints for protein loop modeling as well.

The present work addresses the conformational sampling of particularly flexible compounds, including macrocycles, in comparison to smaller drug-like compounds. This draws on three carefully curated compound sets, called the 'Drug-like set', the 'Flexible set' and the 'Macrocycle set'. The Drug-like set has been presented before,[22,30] but the Flexible and Macrocycle sets were compiled for the present work. Here, the term 'Flexible compound' refers specifically to nonmacrocyclic molecules with at least 12 rotatable bonds, represented by the Flexible set. For every test compound there is at least one good-quality publicly available X-ray structure in complex with a biological macromolecule; the X-ray structure of the bound test compound will be referred to as the bioactive structure. Each set contains a sizable number of compounds (Drug-like: 253, Flexible: 50, Macrocycle: 30), but the emphasis was on selecting the test compounds carefully rather than collating the largest possible sets. Such balance allowed detailed tests of computationally demanding protocols with the Flexible and Macrocycle sets. The investigated sampling methods are comprised of LowModeMD and Stochastic Search implemented in MOE, and LMOD, LLMOD, MT/LMOD, MT/LLMOD and MD/LLMOD in MacroModel. Where applicable, these were explored with three force fields, MMFF,[61] OPLS2005[62] and the recent OPLS2.0.[63] The topic is not high-throughput library generation, but thorough conformational searches for compounds of special interest.

First, the study addresses the ability to 'reproduce' the bioactive X-ray structures, since the performance of computational protocol in that respect with Flexible and Macrocycle compounds was highly uncertain at the outset. Second, we address the conformational coverage, via the number of generated conformers (NbConfs), their compactness/extendedness, and the number of 3D pharmacophores they visit. Since considerable sampling was

performed for each compound, we were able to examine how frequently the global energy minimum was located by independent search runs. It gives an indication regarding the convergence of the searches.

With both MOE and MacroModel, adjustments to the search parameters yield notably better results than obtained at default settings. The rates of reproduction of the bioactive structures, and of location of the global energy minimum, are very encouraging for the Flexible and Macrocycle compounds (and higher for the Drug-like compounds). The computed conformers span a compactness range which typically encompasses the bioactive structure. Therefore the conformational sampling of larger flexible compounds can be tackled with mainstream methods and yields results which should be useful in drug discovery/pharmacology applications.

2. Methods

2.1. Preparation of compound test sets

The sampling protocols were tested with three sets of compound, referred to as the 'Drug-like', 'Flexible', and 'Macrocycle' sets. Each set is relevant to pharmacology and medicinal chemistry, but represents different types of compounds. The Flexible set was assembled to study compounds where the degrees of freedom are mostly contained in noncyclic chains. These sets were curated with care to provide diverse and reliable publicly available X-ray bioactive structures available from the PDB.[64] The PDB and ligand codes for the selected compounds are in Supplementary data (Supplementary Tables S1–S3). Every compound except one (PDB entry 3OMJ) is bound to a protein; the macrocycle in 3OMJ is bound to DNA. All the compounds are bound noncovalently to their target macromolecule.

The Drug-like set contains 253 chemically diverse compounds, which have already been carefully characterized with other methods,[22] and have molecular weight (MW) and number of rotatable bonds in the conventional drug-like range. It provides a reference for comparisons with larger compounds in the Flexible and Macrocycle sets.

The Flexible and Macrocycle sets were compiled from high-quality crystal structures, determined at a resolution of 2 Å or better, and for which the structure factors were deposited in the PDB. If the same compound was crystallized in multiple PDB entries, the entry with the best resolution was kept. All metal containing compounds (e.g. metal chelating porphyrins) were removed, as well as compounds with more than two charged centers at pH 7. Compounds with more than 20 noncyclic nonterminal rotatable bonds were deemed overly flexible and were excluded using the b_1rotN descriptor of MOE, which counts the number of rotatable bonds outside rings. This initial filtering yielded 5133 chemically different compounds, which were split in two sets. The macrocycles were excluded from the first set, from which the Flexible set was selected. The second set was comprised of macrocyclic compounds, from which the Macrocycle set was derived. Here, a macrocycle is defined as a ring of at least 9 atoms.

The Flexible set resulted from further filtering, to extract diverse compounds that are more flexible than conventionally drug-like compounds. Thus, compounds with MOE descriptor opr_nrot <12 were removed, to retain only compounds with $12 \leqslant opr\_nrot \leqslant 20$ (descriptor opr_nrot[65] assigns some flexibility to rings). Compounds bound to DNA were removed. To enrich the set in molecules of pharmaceutical interest, we removed compounds with alkyl chains of four carbons or longer (e.g. lipid-like), or with more than 10 chiral centers. We also removed compounds present multiple times in the same PDB entry, since they tend to be

crystallization agents (e.g. polyethylene glycol). Then, a diversity analysis was performed with MOE on the remaining molecules, combining MACCS fingerprints and the number of rotatable bonds counted with opr_nrot (same weight on each criterion). This short-listed 150 diverse compounds differing regarding (i) their count of rotatable bonds (between 12 and 20), and (ii) their chemical functionalities. From this list, a final set of 50 diverse Flexible compounds bound to 32 diverse protein families was selected (see Supplementary data). Diversity of protein binding sites helps represent diverse bioactive binding modes, for example, regarding their compactness. These X-ray structures were inspected individually. This provided a well-curated set of 50 ligands with high-quality X-ray bioactive structures, called the Flexible set of compounds.

In parallel, molecules with rings of at least 9 atoms were extracted from the above-mentioned 5133 compounds, yielding 86 macrocyclic ligands. Incompletely built macrocycles in the X-ray structures were removed. Compounds with MOE descriptor b_1rotN $\geqslant 10$ were removed, to focus on compounds where the flexibility resides primarily in the macrocycle (b_1rotN ignores rotatable bonds in rings). The remaining molecules were clustered at 70% similarity (Tanimoto index) using the MACCS fingerprints. One member per cluster was kept, and a few molecules deemed unsuitable were discarded upon inspection (e.g. PDB entry 3OTI since it contains a chain of 3 linked sulfur atoms and an overly restricted macrocyclic ring). The macrocycle in PDB entry 3OMJ was kept for the sake of chemical diversity, despite being bound to DNA. The resulting final Macrocycle set consisted of 30 compounds (see Supplementary data) with between 9 and 30 rotatable bonds, as defined by descriptor opr_nrot in MOE.

All compounds were initially prepared with MOE, including assignment of bond orders and standard protonation states at pH 7 ('Wash' function), which were individually checked by manual inspection. The tautomers were assigned to be consistent with the X-ray binding modes. Prior to conformational sampling, all ligands were converted to 2D representations to erase memory of the initial X-ray conformation. However, the R/S stereochemistry of the chiral centers in the bioactive structures was maintained in subsequent conformation searches, to concentrate the study on the torsional degrees of freedom.

2.2. MOE conformational search algorithms

The version 2011.10 of MOE was used. The 2D representation of the compounds was used as input. The present work emphasises the investigation of MOE LowModeMD[34] for thorough conformational search since it is a recent and particularly relevant addition to the MOE tool box. A novel and efficient algorithmic approach to the low-mode search is key to LowModeMD.[34] For comparison, sampling with Stochastic Search was also performed. The Stochastic Search uses random moves of the torsional degrees of freedom, and does not use low-mode moves. The conformers were energy-minimized at the default settings of the program. With every method the search parameters were varied (Section 2.5). The MOE LowModeMD and Stochastic Search were performed with the same parameters, to test the influence of the search algorithm on the results. We call a protocol the combination of a search method and its parameters. For every protocol, three independent runs were performed to assess how the results were affected by the stochastic element of the search.

2.3. MacroModel conformational search methods

MacroModel (BatchMin V9.9) distributed with the version 9.3.5 of Maestro was used. All the generic low-mode based search methods available in MacroModel were investigated. Those are the plain

low-mode search (LMOD), Large-scale low-mode (LLMOD), Mixed torsional/Low-mode (MT/LMOD), and Mixed torsional/Large-scale low-mode (MT/LLMOD). With LMOD and LLMOD only low-mode moves are performed, but low-mode and torsional moves are combined with MT/LMOD and MT/LLMOD. When accessing Macro-Model via the widely used Schrödinger Maestro interface, the default method is MT/LMOD. Thus the present work emphasizes MT/LMOD, especially since our tests confirmed that it is a well-balanced search algorithm. The specialized method 'Macrocycle Conformational Sampling' (termed here MD/LLMOD) was recently added to MacroModel and was also investigated, but is considered separately considering its specialized focus on macrocycles (next section).

Input to MacroModel calculations required compounds in 3D format. The 2D-to-3D conversion was performed with the Schrödinger LigPrep program. With LigPrep we turned off all options generating variant tautomers, stereoisomers and protonation states, since these were already assigned manually to be consistent with the X-ray binding modes (see above). The same force field was used during the LigPrep preparation step and the subsequent conformational searches (Section 2.6). For each protocol (search method combined with particular search parameters), three independent runs were performed to assess how the stochastic aspect of the search affected the results.

The conformers were energy-minimized with the default Polak-Ribiere conjugate gradient method. The convergence criterion was an energy gradient of 0.05 kJmol^{-1}/Å or less. The default number of 500 energy-minimization steps was typically not sufficient to reach convergence, so the number of energy-minimizations iterations was set to 3000 for all generic MacroModel search protocols.

2.4. Specialized MD/LLMOD method for macrocycles

With the Macrocycle set, we also tested a protocol recently proposed by Schrödinger specifically for macrocycles. This protocol is accessible from the MacroModel menu of the Maestro GUI under 'Macrocycle conformational sampling'. Here, we call this protocol MD/LLMOD, based on its two-stage search strategy.

The first stage is a high temperature MD-based simulated annealing, while the second stage is a Large-scale low-mode (LLMOD) search.[43] By default 5000 simulated annealing cycles are performed, starting from a temperature of 1000 K which is then decreased to 300 K, followed by energy minimization. Conformers obtained from the simulated annealing are then subjected to LLMOD (5000 search steps by default), during which the eigenvectors of the Hessian may be calculated on the initial structure only, on each new global energy minimum (default setting), or at each search cycle. Other options includes the force field (OPLS2005 by default), the treatment of electrostatics (*GB* by default), the energy window for saved structures ($\Delta E = 10$ kcal/mol by default), the duplicate RMS threshold (0.75 Å by default) and the torsional treatment of selected bond types with high energy barriers. The present study explored these options with the Macrocycles, except the torsional treatment of selected bond types, which was kept at default.

Although MD/LLMOD is explicitly intended for Macrocycles, it was also applied to the Flexible set of compounds out of curiosity. With MD/LLMOD, only one run per protocol was performed.

2.5. Investigated search parameters which influence the conformational ensemble

We tested multiple protocols for each search method. All methods were first run at their default settings (Table 1). The RMSD between conformers was used for removal of duplicate conformers with MacroModel and MOE. This RMSD criterion is referred to as 'Duplicate RMS' in this study, to avoid confusion with the RMSD between computed conformers and their bioactive X-ray counterpart. In addition, with all methods, only the conformers within a specified energy window (ΔE) above the energy of the lowest energy conformer are kept. ΔE is an important parameter which was investigated, alongside other parameters including (i) the treatment of electrostatic interactions with the solvent, (ii) the maximum number of search iteration (Max-Iterations), and (iii) the maximum number of search moves per rotatable bond (Rot-Steps, only relevant for the MacroModel generic methods).

With MOE, LowModeMD and Stochastic Search were performed with the MMFF94x force field. These methods were tested at energy windows $\Delta E = 7$ (default) or 15 kcal/mol; $\Delta E = 20$ kcal/mol was also explored with LowModeMD. The treatment of electrostatics was either the default distance-dependent dielectric constant

Table 1
Default settings[a] associated with the tested conformational search methods

Software	Search method	Force field	Solvation[b]	Duplicate RMS[c] (Å)	ΔE[d]	Max-Iterations[e]	RotSteps[f]
MOE	LowModeMD	MMFF94x	*Diel*	0.25	7	10,000	NA
	Stochastic Search	MMFF94x	*Diel*	0.25	7	10,000	NA
MacroModel	MT/LMOD[g]	OPLS2005	*GB*	0.50	5	1000	100
	LMOD[h]	OPLS2005	*GB*	0.50	5	1000	100
	LLMOD[i]	OPLS2005	*GB*	0.50	5	1000	100
	MT/LLMOD[j]	OPLS2005	*GB*	0.50	5	1000	100
	MD/LLMOD[k]	OPLS2005	*GB*	0.75	10	5000[l]	NA

NA: not applicable.
^a Settings in MOE and MacroModel.

  ^a Settings in MOE and MacroModel.
  ^b Either a distance-dependent dielectric (*Diel*) or a generalized Born (*GB*) solvation model.
  ^c Root mean square deviation cutoff (Å) applied to remove duplicate conformers; in MacroModel when a root mean square deviation is selected to remove duplicates, the default cutoff is 0.5 Å.
  ^d Allowed conformational energy window (kcal/mol) for the conformers.
  ^e Maximum number of search iterations.
  ^f RotSteps was only applicable to the generic MacroModel protocols, and specifies the maximum number of moves per rotatable bond.
  ^g Mixed torsional/low-mode.
  ^h Low-mode.
  ⁱ Large-scale low-mode.
  ^j Mixed torsional/Large-scale low-mode.
  ^k MD/LLMOD is the specialised method proposed by Schrödinger for macrocycles.
  ^l The number of LLMOD search steps; in addition, 5000 preliminary cycles of MD-based simulated annealing are performed by default. Another option of MD/LLMOD is how frequently the eigenvectors are recalculated for the low-mode moves, which is for each new global energy minimum by default.

7902

I-Jen Chen, N. Foloppe/Bioorg. Med. Chem. 21 (2013) 7898–7920

(*Diel*) or a generalized Born (*GB*) solvation model.[66] The default maximum number of iterations (Max-Iterations = 10,000) and the default Duplicate RMS (0.25 Å) for rejection of similar conformers were kept with MOE, based on previous experience[22] and preliminary tests. Thus, with MOE the Max-Iterations and Duplicate RMS and were kept at 10,000 and 0.25 Å, respectively.

Comparable search parameters were investigated with the MacroModel methods. Each MacroModel search method was first carried out at default settings (Table 1). Then, the varied parameters were the treatment of electrostatic (distance-dependent dielectric *Diel* or generalized Born *GB*), the Duplicate RMS (0.25 or 0.5 Å), Max-Iterations (1000, 5000 or 10,000), RotSteps (100, 200 or 400), and the force field (OPLS2005, OPLS2.0 or MMFFs).

2.6. Energy models

Each sampling protocol was performed with the associated default force field, that is MMFF94x[61] in MOE and OPLS2005[62] with the Schrödinger methods. To test the influence of the force field, some protocols performed with the Schrödinger software were carried out with the OPLS2.0 or the MMFFs force fields. MMFFs and MMFF94x are two largely equivalent variants of the Merck molecular force field.[61] OPLS2.0 is a promising recent development of the OPLS family of force fields,[63] expected to yield more refined energetics than OPLS2005. Only limited work has been published with OPLS2.0, and it is therefore timely to examine how it behaves in broad conformational sampling studies. With the Schrödinger software, the same force field was used when preparing the compounds with LigPrep as when performing the subsequent conformational search.

2.7. Reproduction of the bioactive compound structures

An important test of a conformational sampling protocol is whether it produces at least one conformer close to the corresponding compound bioactive X-ray structure. This was tested by finding the lowest RMSD between the members of a conformational ensemble and the corresponding X-ray bioactive reference (for nonhydrogen atoms only), after best fit of the conformers. Four RMSD thresholds were investigated, within which one may consider the bioactive structure reproduced by a computed conformer, namely 0.5, 1.0, 1.5, and 2.0 Å. The percentage of bioactive structures reproduced by a protocol within a given RMSD threshold is abbreviated as *%BioConf_Rep*. The 1.0 Å threshold is emphasized in the analysis of the results, because it arguably represents a good quality fit of practical value, consistent with previous studies.[22,30,33,46] One should keep in mind, however, that the significance of an RMSD depends on the size of the molecule. An RMSD value of, say 1.0 Å, represents a better performance for a larger than for a smaller compound. The generation of conformers of particular interest was supplemented by more generic tests of the conformational coverage, as described in the next section.

2.8. Conformational coverage assessed by 3D descriptors

An important aspect of conformational sampling is its coverage, that is, how completely and finely the conformational space of a molecule is represented by the computed conformers.[24,38,67,68] A simple measure of coverage is the average number of generated conformers per compound (NbConfs),[22,68] since more conformers represent a more extensive coverage. In addition, the conformational coverage was investigated by 3D descriptors to further characterize the diversity and overall distribution of the conformers. The radius of gyration Rgyr was used to quantify the range of compactness of the conformers, and was calculated with MOE as before.[22,30] Rgyr distributions, represented as boxplots, were

compared between selected sampling protocols. Rgyr was also obtained for every compound X-ray bioactive structure (Rgyr_X-ray). These Rgyr_X-ray were compared to the minimum (Rgyr_min) and maximum (Rgyr_max) Rgyr values for the computed conformers, to investigate if Rgyr_X-ray is within the range of computed Rgyr.

The conformational diversity of computed ensembles can be assessed with the number of corresponding three-point 3D pharmacophores visited by the ensemble.[22,24,27,30] This approach was applied with three-point pharmacophores defined with the Schrödinger Canvas chemoinformatics software, using the six features hydrogen-bond acceptor, hydrogen-bond donor, hydrophobic, negative charge, positive charge and aromatic ring. The distances between features were categorized in 2 Å bins [0, 2[, [2, 4[, [4, 6[, ..., [20, infinity[; this range is suitable in view of the Rgyr distributions. The visited 3D-pharmacophores were stored in fingerprints calculated with Canvas. Such fingerprint captures all the three-point pharmacophores visited by a selected conformational ensemble, each pharmacophore corresponding to a distinct 'bit'. Each bit encodes the specific pharmacophoric features and the distances between them. This allows to count all the 3D pharmacophores visited by each conformational ensemble. When three searches were run per protocol (see above), the 3D pharmacophores generated by the three runs were merged, and every visited pharmacophore was counted only once. Hence, this procedure yields the total number of distinct nonredundant pharmacophores generated by a search protocol, which is a quantitative estimate of the sampling of the pharmacophoric space, and of the coverage of the underlying conformational diversity. This total number of nonredundant pharmacophores is referred to as the total number of visited pharmacophores per protocol. This analysis was applied to both the MacroModel and the MOE outputs.

2.9. Global energy minima and convergence of the searches

Since the investigated search methods proceed by stochastic moves, it is important to assess their convergence. In that respect, the ability of a search protocol to consistently locate the global minimum of the conformational energy surface plays a special role.[22,38,69] The ability to find the global energy minimum is a convergence criterion of special interest, considering its importance for the physical characterization of a compound. There is no guarantee that a stochastic search will sample all the regions of conformational space, so it could miss the global energy minimum. However, the search parameters can be adjusted to augment the search and increase the likelihood that it finds the global energy minimum. Thus, a test of the convergence is whether or not several independent runs (with the same protocol) consistently find the global energy minimum. One notes that this is a simplified test of convergence. In theory, a more stringent test would examine if all energy minima have been found in repeated runs, but that is hardly feasible in practice. However, the frequency of sampling of the global minimum is already a very useful indication, if only because finding the global minimum is a necessary condition for convergence. The ability to find the global energy minimum is also another test of coverage.

First, one has to identify a plausible global energy minimum per compound. The only practical approach is to accumulate enough sampling so that it is highly likely that the global energy minimum has been located. Here, we took advantage of the many search runs performed with the same energy model across protocols for each compound. In aggregation, these numerous searches are highly likely to locate the global energy minimum for the associated energy model.

With MacroModel, the searches analyzed with respect to the global energy minimum were those performed with *GB* and

OPLS2005. The global energy minimum was defined as the lowest energy conformer across 36 aggregated runs for the Drug-like set, 39 aggregated runs for the Flexible set, and 24 aggregated runs for the Macrocycles. With MOE, the runs analyzed with respect to the global energy minimum were those performed with *GB* and MMFF94x. The LowModeMD and Stochastic Search runs were

Figure 1. Examples of compounds in the Drug-like set, with the associated PDB codes and Oprea number of rotatable bonds (opr_nrot, see Fig. 4A). The full set contains 253 compounds.

aggregated, corresponding to 12, 15 and 15 aggregated runs for the Drug-like, Flexible and Macrocycle sets, respectively. Again, the global energy minimum was defined as the lowest energy conformer across the aggregated runs. Thus, for every compound, the global energy minimum was identified for the MOE GB/MMFF94x and for the MacroModel GB/OPLS2005 energy models.

The global energy minimum for every compound was used to examine how frequently it was found by selected protocols. A search may not find exactly the global energy minimum, but an equivalent conformer very close in energy and structure. Finding such conformer similar to the global energy minimum was deemed equivalent to finding the global energy minimum. Thus, a conformer was considered akin to the global energy minimum if it was within 0.5 kcal/mol and 0.5 Å of this global minimum. Then, individual search runs were examined to determine the percent of compounds for which they found the global energy minimum (%GlobMin_found). Since three independent runs were performed per protocol, one can compare the %GlobMin_found values across runs, to examine the consistency with which the global energy minimum was located.

Figure 2. Examples of compounds in the Flexible set, with the associated PDB codes and Oprea number of rotatable bonds (opr_nrot, see Fig. 4A). The full set contains 50 compounds.

I-Jen Chen, N. Foloppe / Bioorg. Med. Chem. 21 (2013) 7898–7920

7905

1W96   opr_nrot = 16

2VW5   opr_nrot = 16

1BXO   opr_nrot = 20

1WAW   opr_nrot = 20

2XBK   opr_nrot = 20

2IYA   opr_nrot = 23

3OMJ   opr_nrot = 24
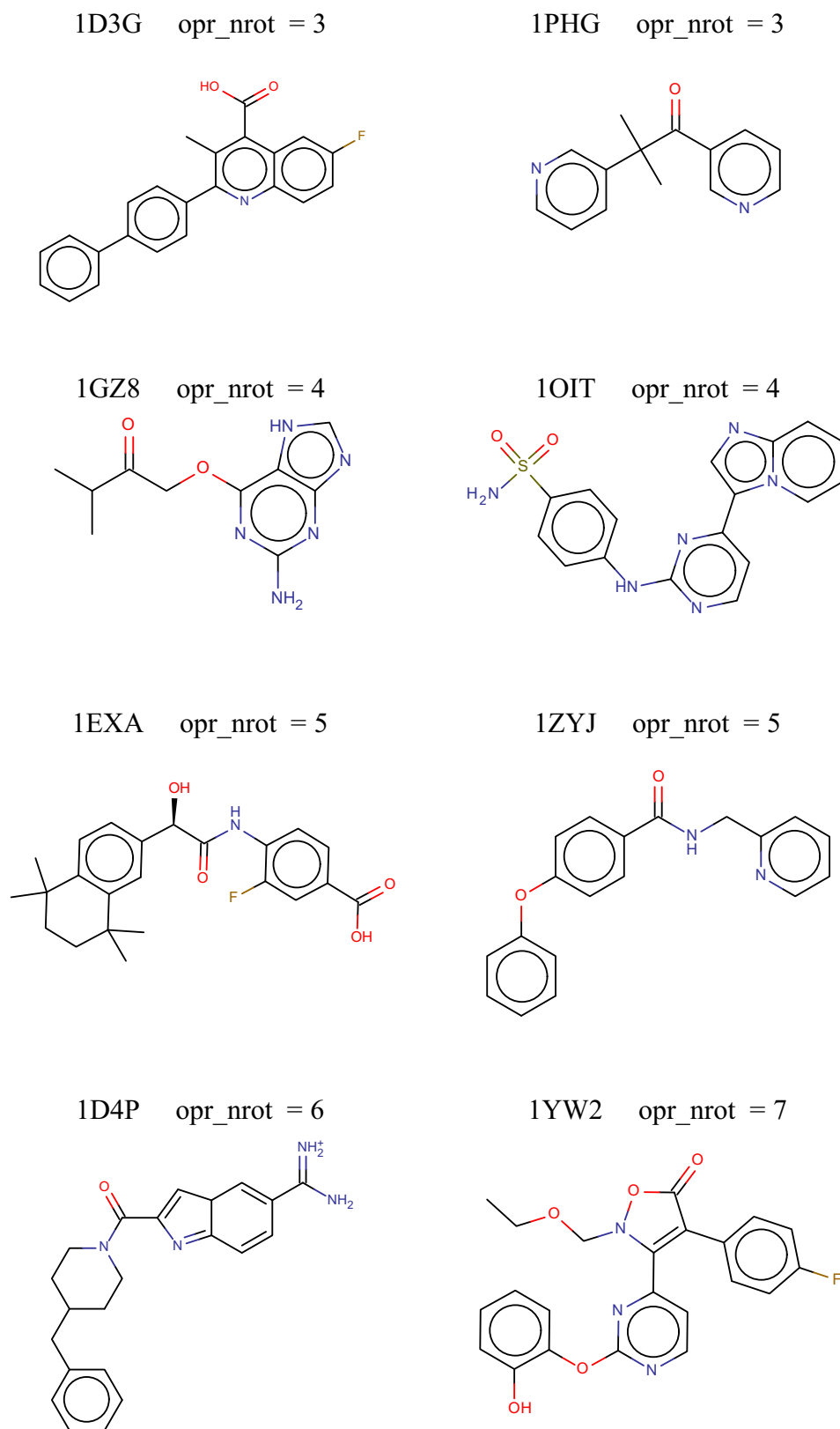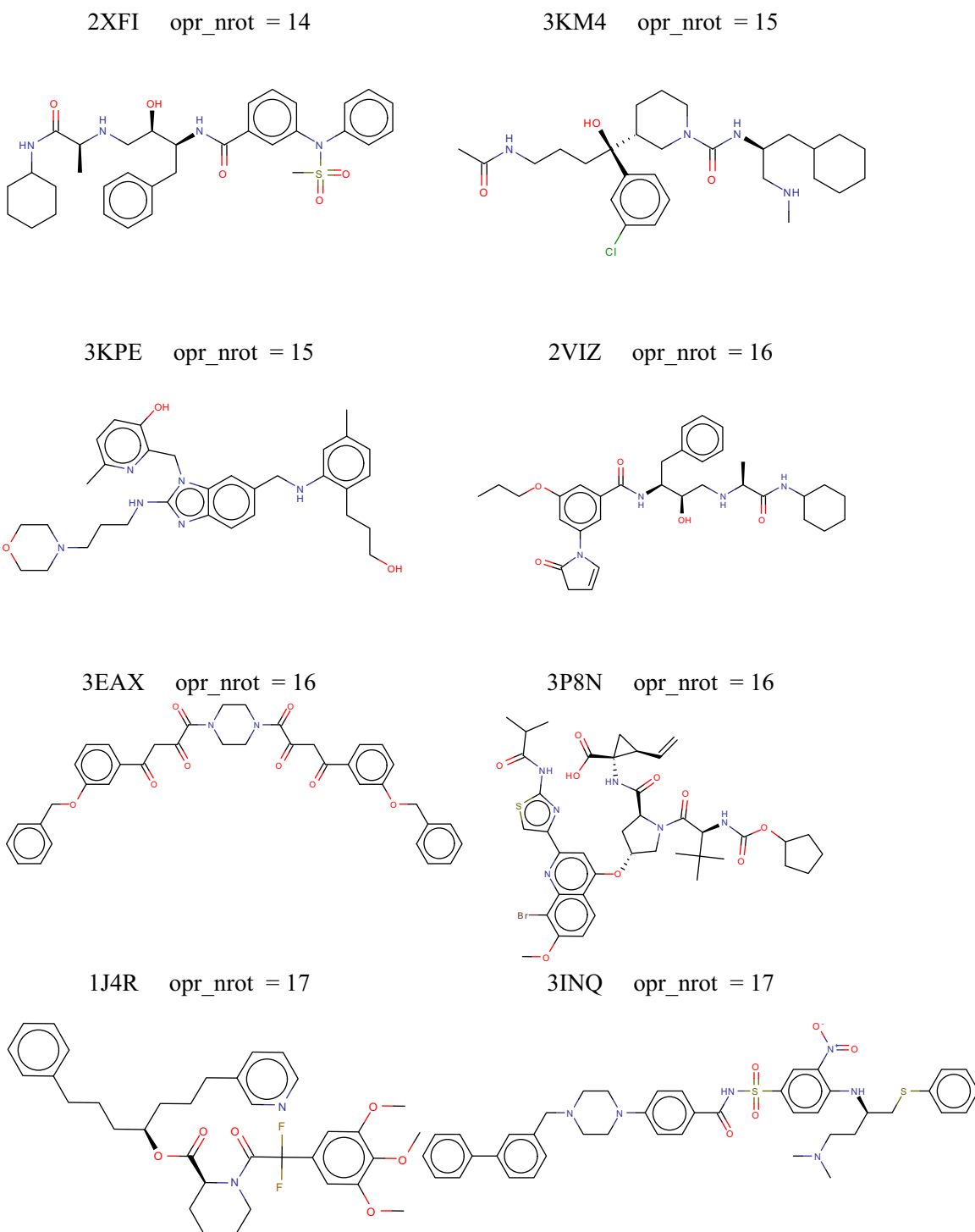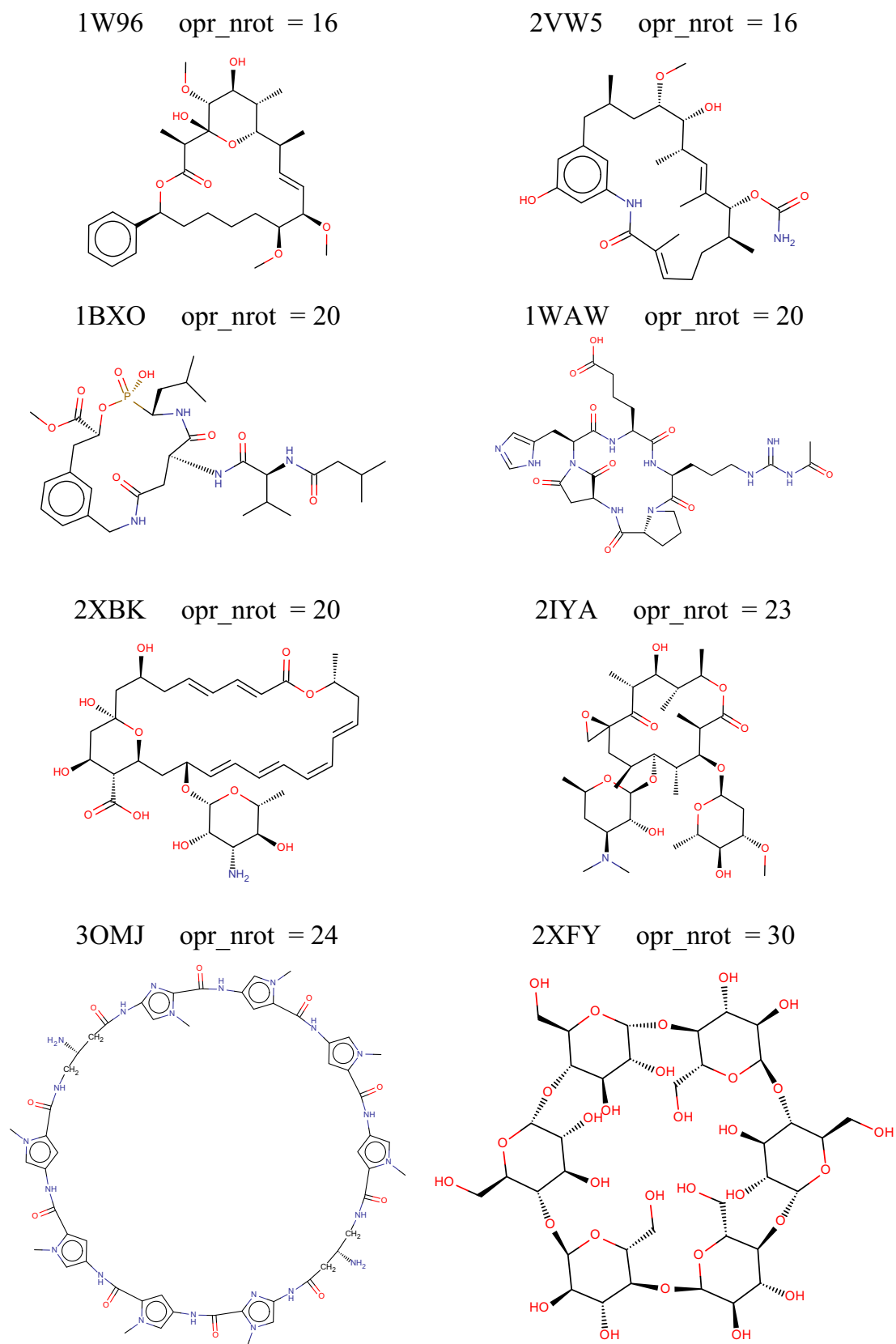
2XFY   opr_nrot = 30

Figure 3. Examples of compounds in the Macrocycle set, with the associated PDB codes and Oprea number of rotatable bonds (opr_nrot, see Fig. 4A). The full set contains 30 compounds.

3. Results and discussion

3.1. Properties of the compound sets

This study investigated the performance of mainstream conformational sampling methods with three compound sets of different characteristics (see Section 2). These sets were tailored to cover different flexibility ranges relevant to drug discovery. They are the 'Drug-like' (253 compounds), the 'Flexible' (50 compounds), and the 'Macrocycle' (30 compounds) sets. Examples of these compounds are shown in Figures 1–3. The compound sets are compared in Figure 4 with respect to their number of Oprea rotatable bonds,[65] number of chiral centres and molecular weight.

Figure 4A shows that the compounds of the Flexible and Macrocycle sets have more rotatable bonds than those in the Drug-like set. The number of rotatable bonds ranged from 1 to 13 for the Drug-like set, from 12 to 17 for the Flexible set, and from 9 to 30 for the Macrocycle set. Compounds in the Flexible and Macrocycle sets also have more chiral centers than the 'Drug-like' set (Fig. 4B). These chiral centers were kept constrained to their configuration in the bioactive structures, to avoid facing an unmanageable number of chiral classes, and focus the analysis of the torsional flexibility. This, however, is a reminder that in true discovery situations the search space with complex compounds may have to include chiral centers, and would be even larger than considered here. Overall, the three curated compound sets provide a broad basis for a robust assessment of conformational sampling algorithms.

3.2. Overview of tested search protocols

The primary goal is to address the Flexible and Macrocycle compounds, but results on the Drug-like compounds are presented first (Section 3.3) to put the Flexible and Macrocycle compounds in perspective. Every search method was first tested at its default settings (Table 1 and Section 2). Then the search parameters were adjusted, while maintaining computational tractability. We call a protocol the combination of a search method with specific values of the search parameters. In total, 22 protocols were tested for the Drug-like set (Table 2), 25 with the Flexible set (Table 3) and 34 with the Macrocycle set (Tables 4 and 5). Except with MD/LLMOD, each protocol was run independently three times to address the expected variation resulting from the stochastic character of the searches. For the protocols run three times, the percentage of reproduced bioactive structures (%BioConf_Rep) values are presented with their mean and standard deviation (SD) across the three runs (Tables 2–4). The variation for %BioConf_Rep and NbConfs was typically small, so these properties were not strongly affected by the stochastic character of the searches. This is in itself an important observation, which gives confidence that the mean %BioConf_Rep values are representative and a sound basis for comparison across protocols. For each search method, the combination of parameters which yielded the best performance is referred to as the 'enhanced' protocol for the method.

	Average values of properties		
Compound set	Drug-like	Flexible	Macrocycle
Molecular Weight	373	558	576
b_1rotN	5	12	3
opr_nrot	6	13	16
Chiral centers	0.6	2	8
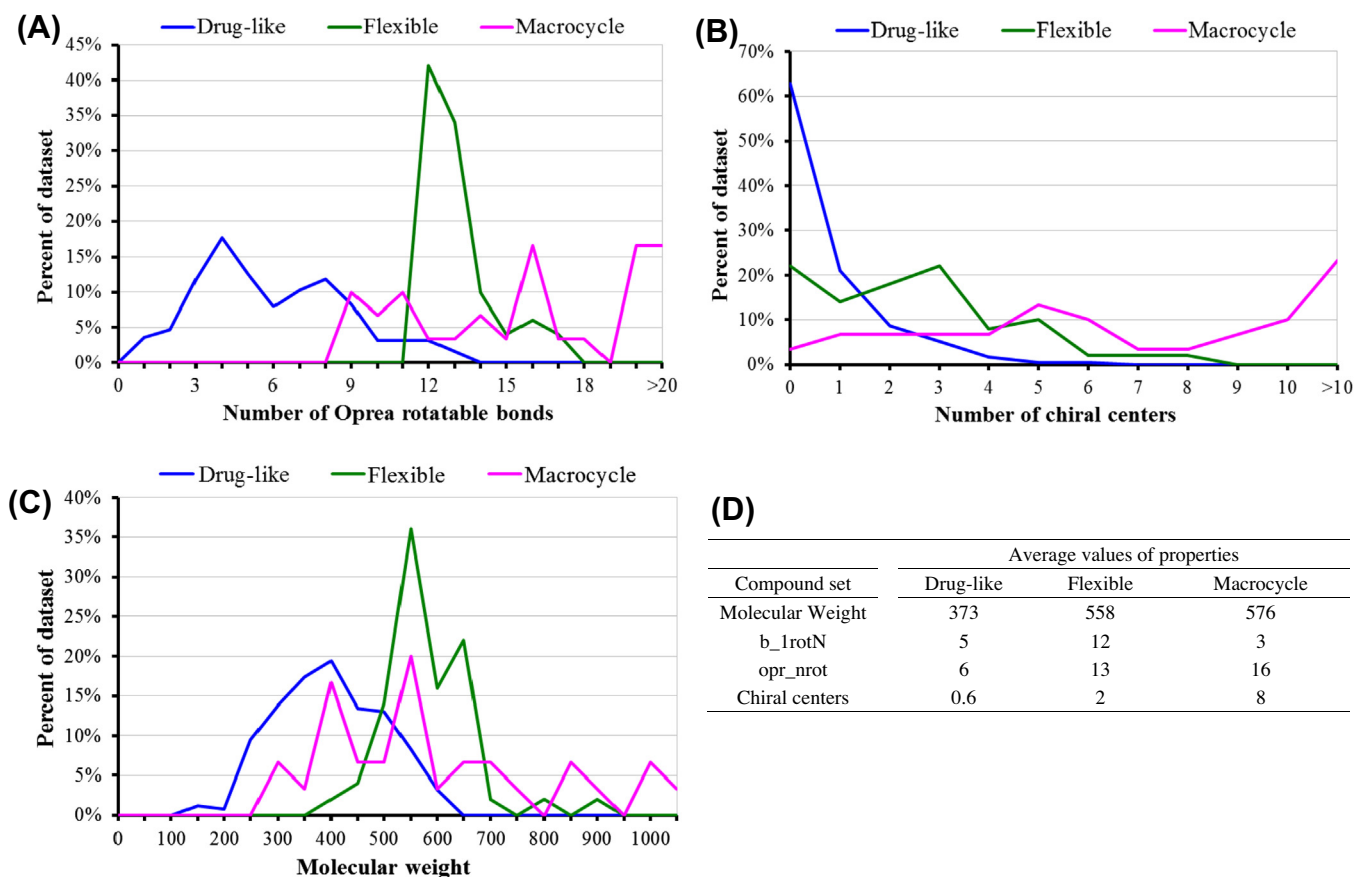
Figure 4. Distribution of properties characterizing the flexibility and size of the molecules in the Drug-like (blue), Flexible (green) and Macrocycle (magenta) compound sets. The properties are the number of Oprea rotatable bond (panel A), the number of chiral centers (panel B) and the molecular weight (panel C). In each panel, the distributions are reported in percent of each compound set. The mean values are summarized in panel D. The number of Oprea rotatable bond per compound (panel A) was counted using the descriptor 'opr_nrot' as implemented in MOE, inspired from the work of Oprea.[65] This descriptor not only counts exocyclic non-terminal rotatable single bonds, but also assigns some flexibility to aliphatic rings. In MOE, opr_nrot counts one rotatable bonds per 5-membered ring, two rotatable bonds per 6-membered rings, and so on up to 8-membered rings. For 9-membered rings and above, opr_nrot counts as rotatable all single bonds not shared with other rings. Here, macrocycles are considered to be rings formed of at least 9 atoms. In panel A, the 5 macrocycles with opr_nrot >20 are aggregated under the same rightmost point.

Table 2
Protocols[a] and performance[b] for reproduction of the X-ray bioactive structures of ligands in the Drug-like set[c]

Protocol	Investigated parameters								%BioConf_Rep[i] (%) RMSD (Å) versus bioactive				NbConfs[j]
	ΔE[d]	Solvation model[e]	Duplicate RMS[f]	Force field	Max-Iteration[g]	RotSteps[h]		0.5	1.0	1.5	2.0	
MOE LowModeMD	7	*Diel*	**0.25**	**MMFF94x**	**10,000**	NA	Mean	38	77	87	94	156
							SD	0	1	0	0	3
	7	*GB*	0.25	MMFF94x	10,000	NA	Mean	46	91	98	100	304
							SD	1	0	1	0	10
	15	*GB*	0.25	MMFF94x	10,000	NA	Mean	46	94	100	100	755
							SD	0	0	0	0	8
MOE Stochastic	**7**	***Diel***	**0.25**	**MMFF94x**	**10,000**	NA	Mean	38	77	85	93	139
							SD	0	0	1	0	1
	7	*GB*	0.25	MMFF94x	10,000	NA	Mean	45	90	97	100	302
							SD	0	1	0	0	1
	15	*GB*	0.25	MMFF94x	10,000	NA	Mean	45	94	98	100	705
							SD	1	1	1	0	11
MacroModel MT/LMOD[k]	**5**	***GB***	**0.50**	**OPLS2005**	**1000**	**100**	Mean	49	89	97	99	101
							SD	1	2	0	0	0
	5	*Diel*	0.50	OPLS2005	1000	100	Mean	41	73	81	87	55
							SD	1	0	1	0	0
	5	*GB*	0.25	OPLS2005	1000	100	Mean	53	89	95	98	159
							SD	1	0	0	1	1
	5	*GB*	0.50	OPLS2005	10,000	100	Mean	48	90	96	98	107
							SD	0	1	0	0	1
	15	*GB*	0.50	OPLS2005	1000	100	Mean	55	92	98	100	194
							SD	2	3	3	0	1
	15	*GB*	0.25	OPLS2005	10,000	100	Mean	55	92	98	100	345
							SD	2	3	3	0	1
	15	*GB*	0.25	OPLS2005	10,000	400	Mean	65	97	100	100	1032
							SD	0	1	0	0	1
	5	*GB*	0.50	OPLS2.0	1000	100	Mean	48	88	96	98	101
							SD	1	1	1	0	0
	15	*GB*	0.25	OPLS2.0	10,000	100	Mean	57	92	99	100	347
							SD	2	1	0	0	1
	15	*GB*	0.25	MMFFs	10,000	100	Mean	48	93	99	100	306
							SD	2	1	0	0	0
MacroModel LMOD[l]	**5**	***GB***	**0.50**	**OPLS2005**	**1000**	**100**	Mean	43	78	87	95	75
							SD	1	0	1	1	0
	15	*GB*	0.25	OPLS2005	10,000	100	Mean	53	89	95	99	274
							SD	1	0	1	0	1
MacroModel LLMOD[m]	**5**	***GB***	**0.50**	**OPLS2005**	**1000**	**100**	Mean	39	67	79	90	41
							SD	3	2	1	1	0
MacroModel MT/LLMOD[n]	**5**	***GB***	**0.50**	**OPLS2005**	**1000**	**100**	Mean	48	89	96	98	101
							SD	2	1	1	0	1
	15	*GB*	0.25	OPLS2005	10,000	100	Mean	57	94	99	100	368
							SD	1	0	0	0	0
	15	*GB*	0.25	OPLS2005	10,000	400	Mean	65	97	100	100	1112
							SD	1	1	0	0	1

NA: not applicable.

[a] Default protocols are in bold.
[b] Measured as the percentage of reproduced bioactive structures (*%BioConf_Rep*) within a given RMSD threshold.
[c] The 253 compounds of the Drug-like set.
[d] Allowed relative conformational energy window (kcal/mol) for the conformers.
[e] Distance-dependent dielectric (*Diel*) or generalized Born (*GB*) solvation model.
[f] Root Mean square deviation cutoff (Å) to remove duplicate conformers.
[g] Maximum total number of search iterations.
[h] RotSteps was only applicable to the MacroModel protocols, and specifies the maximum number of moves per rotatable bond.
[i] *%BioConf_Rep* is the percent of bioactive X-ray structures reproduced by a computational protocol, within an RMSD threshold (0.5, 1.0, 1.5 or 2.0 Å).
[j] NbConfs is the average number of conformers per compound output by a search run. Each *%BioConf_Rep* and NbConfs value is reported as the mean across 3 independent search runs, alongside the corresponding standard deviation (SD).
[k] Mixed torsional/low-mode.
[l] Low-mode.
[m] Large-scale low-mode.
[n] Mixed torsional/Large scale low-mode.

3.3. Reproduction of bioactive structures with the drug-like set of compounds

With the drug-like compounds, *%BioConf_Rep* and NbConfs values are summarized in Table 2. *%BioConf_Rep* for selected protocols is compared graphically in Figure 5. We first describe the results obtained with MOE, followed by those obtained with MacroModel. The default LowModeMD protocol (ΔE = 7 and *Diel*) gave *%BioConf_Rep* = 77% within RMSD ≤ 1.0 Å, and 94% within RMSD ≤ 2.0 Å. Replacing *Diel* by *GB* with LowModeMD (keeping ΔE = 7) increased *%BioConf_Rep* to 91% (RMSD ≤ 1.0 Å). The NbConfs values show that *GB* solvation expands the sampled conformational space, with almost twice more conformers generated with *GB* than with the default *Diel*. However, increasing NbConfs further by

Table 3
Protocols[a] and performance[b] for reproduction of the X-ray bioactive structures of ligands in the Flexible set[c]

Protocol	Investigated parameters							%BioConf_Rep[i] (%) RMSD (Å) versus bioactive				NbConfs[j]
	ΔE[d]	Solvation Model[e]	Duplicate RMS[f]	Force field	Max-Iteration[g]	RotSteps[h]		0.5	1.0	1.5	2.0	
MOE LowModeMD	**7**	***Diel***	**0.25**	**MMFF94x**	**10,000**	NA	Mean	0	9	35	63	408
							SD	0	2	2	1	20
	7	GB	0.25	MMFF94x	10,000	NA	Mean	5	47	86	95	1853
							SD	1	1	2	1	60
	15	GB	0.25	MMFF94x	10,000	NA	Mean	5	68	97	98	5448
							SD	1	2	1	0	75
	20	GB	0.25	MMFF94x	10,000	NA	Mean	5	70	96	98	5712
							SD	1	2	2	0	118
MOE Stochastic	**7**	***Diel***	**0.25**	**MMFF94x**	**10,000**	NA	Mean	2	7	29	59	236
							SD	0	1	5	5	2
	7	GB	0.25	MMFF94x	10,000	NA	Mean	5	41	79	88	1312
							SD	1	3	1	3	84
	15	GB	0.25	MMFF94x	10,000	NA	Mean	8	59	93	95	3986
							SD	0	4	3	3	154
MacroModel MT/LMOD[k]	**5**	***GB***	**0.50**	**OPLS2005**	**1000**	**100**	Mean	1	20	59	89	205
							SD	1	4	6	2	6
	5	Diel	0.50	OPLS2005	1000	100	Mean	0	2	19	41	87
							SD	0	0	4	8	3
	15	GB	0.50	OPLS2005	1000	100	Mean	1	40	78	97	511
							SD	1	4	2	1	6
	15	GB	0.25	OPLS2005	10,000	100	Mean	5	45	87	98	1159
							SD	1	1	2	2	8
	15	GB	0.25	OPLS2005	20,000	100	Mean	3	44	90	99	1178
							SD	3	2	2	1	28
	20	GB	0.25	OPLS2005	10,000	100	Mean	7	45	90	99	1206
							SD	2	4	2	1	3
	15	GB	0.25	OPLS2005	10,000	200	Mean	9	55	91	100	2281
							SD	1	5	3	0	5
	15	GB	0.25	OPLS2005	10,000	400	Mean	7	65	95	100	4452
							SD	1	2	1	0	16
	5	GB	0.50	OPLS2.0	1000	100	Mean	0	22	63	83	206
							SD	0	8	1	1	6
	15	GB	0.25	OPLS2.0	10,000	100	Mean	2	41	84	98	1188
							SD	2	6	5	0	1
	15	GB	0.25	OPLS2.0	10,000	400	Mean	7	59	98	98	4519
							SD	1	3	0	0	18
	15	GB	0.25	MMFFs	10,000	100	Mean	6	43	90	97	1142
							SD	2	1	4	1	3
MacroModel LMOD[l]	**5**	***GB***	**0.50**	**OPLS2005**	**1000**	**100**	Mean	1	7	28	63	143
							SD	1	2	7	2	3
	15	GB	0.25	OPLS2005	10,000	100	Mean	2	25	59	89	856
							SD	2	2	8	1	9
MacroModel LLMOD[m]	**5**	***GB***	**0.5**	**OPLS2005**	**1000**	**100**	Mean	1	10	23	53	77
							SD	1	5	3	1	2
MacroModel MT/ LLMOD[n]	**5**	***GB***	**0.5**	**OPLS2005**	**1000**	**100**	Mean	2	25	58	86	195
							SD	2	5	4	4	1
	15	GB	0.25	OPLS2005	10,000	100	Mean	6	53	90	99	1291
							SD	3	6	2	1	10
	15	GB	0.25	OPLS2005	10,000	400	Mean	11	65	97	100	4950
							SD	2	2	1	0	13
MD/LLMOD[o]	**10**	***GB***	**0.75**	**OPLS2005**	**5000**	NA		0	50	78	94	1093

NA: not applicable.
[a] Default protocols are in bold.
[b] Measured as the percentage of reproduced bioactive structures (%BioConf_Rep) within a given RMSD threshold.
[c] The 50 compounds of the Flexible set.
[d] Allowed relative conformational energy window (kcal/mol) for the conformers.
[e] Distance-dependent dielectric (Diel) or generalized Born (GB) solvation model.
[f] Root mean square deviation cutoff (Å) to remove duplicate conformers.
[g] Maximum number of search iterations.
[h] RotSteps was only applicable to the MacroModel protocols, and specifies the maximum number of moves per rotatable bond.
[i] %BioConf_Rep is the percent of bioactive X-ray structures reproduced by a computational protocol, within an RMSD threshold (0.5, 1.0, 1.5 or 2.0 Å).
[j] NbConfs is the average number of conformers per compound output by a search run. Each %BioConf_Rep and NbConfs value is reported as the mean across 3 independent search runs, alongside the corresponding standard deviation (SD), except for MD/LLMOD.
[k] Mixed torsional/Low-mode.
[l] Low-mode.
[m] Large-scale low-mode.
[n] Mixed torsional/Large-scale low-mode.
[o] MD/LLMOD is the Schrödinger specialized protocol for macrocycles.

I-Jen Chen, N. Foloppe / Bioorg. Med. Chem. 21 (2013) 7898–7920

7909

Table 4

Protocols[a] and performance[b] for reproduction of the X-ray bioactive structures of ligands in the Macrocycle set[c]

Protocol	Investigated parameters							%BioConf_Rep[i] (%) RMSD (Å) versus bioactive				NbConfs[j]
	ΔE[d]	Solvation Model[e]	Duplicate RMS[f]	Force field	Max-Iteration[g]	RotSteps[h]		0.5	1.0	1.5	2.0	
MOE LowModeMD	**7**	***Diel***	**0.25**	**MMFF94x**	**10,000**	NA	Mean	29	49	68	80	61
							SD	2	2	5	3	2
	7	*GB*	0.25	MMFF94x	10,000	NA	Mean	33	56	80	86	188
							SD	0	2	3	2	20
	15	*GB*	0.25	MMFF94x	10,000	NA	Mean	34	72	84	89	1675
							SD	2	7	2	2	71
	20	*GB*	0.25	MMFF94x	10,000	NA	Mean	32	72	83	90	2347
							SD	2	2	3	3	51
MOE Stochastic	**7**	***Diel***	**0.25**	**MMFF94x**	**10,000**	NA	Mean	23	39	56	66	26
							SD	4	1	3	1	6
	7	GB	0.25	MMFF94x	10,000	NA	Mean	30	52	56	70	74
							SD	4	6	6	2	9
	15	GB	0.25	MMFF94x	10,000	NA	Mean	30	53	60	72	479
							SD	2	4	2	6	31
MacroModel MT/LMOD[k]	**5**	***GB***	**0.50**	**OPLS2005**	**1000**	**100**	Mean	23	49	66	79	48
							SD	6	7	7	5	1
	5	Diel	0.50	OPLS2005	1000	100	Mean	29	37	56	67	28
							SD	2	3	4	6	1
	15	GB	0.50	OPLS2005	1000	100	mean	26	59	87	93	855
							SD	2	2	3	0	29
	15	GB	0.25	OPLS2005	10,000	100	Mean	32	64	87	93	855
							SD	5	2	3	0	29
	20	GB	0.25	OPLS2005	10,000	100	Mean	34	64	89	94	952
							SD	5	2	2	2	4
	15	GB	0.25	OPLS2005	10,000	200	Mean	38	66	93	98	1560
							SD	4	2	3	2	38
	15	GB	0.25	OPLS2005	10,000	400	Mean	39	79	96	97	2415
							SD	2	2	2	0	53
	5	GB	0.50	OPLS2.0	1000	100	Mean	27	40	69	82	52
							SD	3	7	5	2	4
	15	GB	0.25	OPLS2.0	10,000	100	Mean	34	72	92	96	906
							SD	4	2	2	4	12
	15	GB	0.25	OPLS2.0	10,000	400	Mean	40	73	93	97	2528
							SD	3	6	0	3	25
	15	GB	0.25	MMFFs	10,000	100	Mean	32	64	90	94	720
							SD	4	4	0	2	28
MacroModel LMOD[l]	**5**	***GB***	**0.50**	**OPLS2005**	**1000**	**100**	Mean	19	40	58	77	40
							SD	2	3	5	9	2
	15	GB	0.25	OPLS2005	10,000	100	Mean	32	56	83	91	782
							SD	2	4	0	2	11
MacroModel MT/ LLMOD[m]	**5**	***GB***	**0.50**	**OPLS2005**	**1000**	**100**	Mean	24	46	58	73	37
							SD	2	4	5	9	2
	15	GB	0.25	OPLS2005	10,000	400	Mean	40	77	92	94	2123
							SD	3	6	2	4	62

NA: not applicable.

[a] Default protocols are in bold; results obtained with the Schrödinger MD/LLMOD protocols are given in Table 5.

[b] Measured as the percentage of reproduced bioactive structures (%BioConf_Rep) within a given RMSD threshold.

[c] The 30 compounds of the Macrocycle set.

[d] Allowed relative conformational energy window (kcal/mol) for the conformers.

[e] Distance-dependent dielectric (Diel) or a generalized Born (GB) solvation model.

[f] Root mean square deviation cutoff (Å) to remove duplicate conformers.

[g] Maximum number of search iterations.

[h] RotSteps was only applicable to the MacroModel protocols, and specifies the maximum number of moves per rotatable bond.

[i] %BioConf_Rep is the percent of bioactive X-ray structures reproduced by a computational protocol, within an RMSD threshold (0.5, 1.0, 1.5 or 2.0 Å).

[j] NbConfs is the average number of conformers per compound output by a search run. Each %BioConf_Rep and NbConfs value is reported as the mean across 3 independent computational runs, alongside the corresponding standard deviation (SD).

[k] Mixed torsional/Low-mode.

[l] Low-mode.

[m] Mixed torsional/Large-scale low-mode search.

widening ΔE from 7 to 15 kcal/mol (keeping *GB*) only yielded a modest further increase in %BioConf_Rep, from 91% to 94%. Adopting a RMSD threshold of 2.0 Å, 100% of the bioactive structures are reproduced by LowModeMD with *GB* and ΔE = 7 or ΔE = 15.

The results from the MOE Stochastic Search closely mirrored those from LowModeMD (Table 2). There was hardly any difference in %BioConf_Rep between LowModeMD and Stochastic Search when performed at same settings. The benefit of applying *GB* solvation was also clear with the Stochastic Search (ΔE = 7, RMSD $\leqslant$ 1.0 Å), increasing %BioConf_Rep by 13% above its value with the default *Diel* setting. The limited impact of increasing the energy window from 7 to 15 kcal/mol was also observed with Stochastic Search. So, LowModeMD or Stochastic Search with *GB* and ΔE = 7 are reasonable compromises for thorough searches of Drug-like

Table 5
MD/LLMOD protocols[a] and performance[b] for reproduction of the X-ray bioactive structures of ligands in the Macrocycle set[c]

		Investigated parameters					%BioConf_Rep[k]				NbConfs[l]
					LLMOD[h]		RMSD (Å) versus bioactive				
ΔE[d]	Solvation model[e]	Duplicate RMS[f]	Force field	MD cycles[g]	Eigenvector[i]	Search steps[j]	0.5 (%)	1.0 (%)	1.5 (%)	2.0 (%)	
10	**GB**	**0.75**	**OPLS2005**	**5000**	**Global_min**	**5000**	**37**	**77**	**93**	**97**	**297**
10	GB	0.75	OPLS2005	5000	Initial_only	5000	27	67	90	97	269
10	GB	0.75	OPLS2005	5000	Every_step	5000	43	73	93	97	362
10	GB	0.75	OPLS2005	5000	Global_min	10,000	37	77	93	97	311
10	GB	0.75	OPLS2005	0	Global_min	5000	37	60	83	90	176
10	Diel	0.75	OPLS2005	5000	Global_min	5000	30	63	87	93	364
10	GB	0.25	OPLS2005	5000	Global_min	5000	43	73	93	97	1022
15	GB	0.75	OPLS2005	5000	Global_min	5000	37	77	97	97	591
15	GB	0.25	OPLS2005	5000	Global_min	10,000	47	80	97	97	1758
30	GB	0.25	OPLS2005	5000	Global_min	10,000	43	77	100	100	2469
10	GB	0.75	OPLS2.0	5000	Global_min	5000	37	67	90	90	328
10	GB	0.75	MMFFs	5000	Global_min	5000	33	67	97	97	247

[a] MD/LLMOD is the Schrödinger specialized method for macrocycles; its default settings are in bold.
[b] Measured as the percentage of reproduced bioactive structures (%BioConf_Rep) within a given RMSD threshold.
[c] The 30 compounds of the Macrocycle set.
[d] Allowed relative conformational energy window (kcal/mol) for the conformers.
[e] Distance-dependent dielectric (Diel) or a generalized Born (GB) solvation model.
[f] Root mean square deviation cutoff (Å) to remove duplicate conformers.
[g] Number of MD-based simulated annealing cycles.
[h] Parameters of the Large-scale low-mode search.
[i] Frequency with which the eigenvectors are recalculated during the LLMOD search: for every new global energy minimum found (Global_min), for the initial conformer only (Initial_only), or at every LLMOD search step (Every_step).
[j] Number of LLMOD search steps.
[k] %BioConf_Rep is the percent of bioactive X-ray structures reproduced by a computational protocol, within an RMSD threshold (0.5, 1.0, 1.5 or 2.0 Å).
[l] NbConfs is the average number of conformers per compound output by a search run.

compounds, although there is a chance that they would miss a bioactive binding mode which could otherwise be found at $\Delta E = 15$. At the RMSD threshold of 2.0 Å, the Stochastic Search with GB also reproduced 100% of the Drug-like bioactive structures. Thus, for compounds of limited flexibility represented by the Drug-like set, no performance difference was observed between LowModeMD and Stochastic Search according to %BioConf_Rep. For the Drug-like set, all MOE search methods reproduced at least 75% of the bioactive structures within 1 Å, and up to 94% with enhanced search parameters. However, LowModeMD produced more conformers than Stochastic Search, especially with GB and $\Delta E = 15$ (Table 2). Therefore, despite virtually identical %BioConf_Rep values, the underlying conformational ensembles generated by LowModeMD and Stochastic Search differ, with LowModeMD affording greater conformational coverage when assessed by NbConfs.

We now turn to the results produced by the low-mode based methods of MacroModel (see Section 2) for the Drug-like set with OPLS2005 (Table 2). MT/LMOD was also tested with OPLS2.0 and MMFFs, but changing the force field had little effect on %BioConf_Rep or NbConfs. In addition to the default settings (Table 1), the parameters were adjusted to be comparable to those which yielded the best %BioConf_Rep value in MOE ($\Delta E = 15$, GB, Duplicate RMS = 0.25 Å, Max-Iteration = 10,000). Considering %BioConf_Rep, MT/LMOD performed similarly to MT/LLMOD. The plain LMOD and LLMOD performed less well than their counterparts with added torsional moves. For example, LMOD gave only %BioConf_Rep = 78% (RMSD $\leqslant$ 1 Å), compared to %BioConf_Rep = 89% with MT/LMOD, maybe because LMOD generated fewer conformers (Table 2). Thus, our results confirm that MT/LMOD is appropriate as the default sampling method in MacroModel for Drug-like compounds. The following analysis emphasizes MT/LMOD.

Within RMSD $\leqslant$ 1.0 Å, MT/LMOD reproduced 88% to 92% of bioactive structures with $\Delta E = 5$ or $\Delta E = 15$, respectively. Thus, MT/LMOD yielded %BioConf_Rep values similar to those obtained with LowModeMD or Stochastic Search with GB and $\Delta E = 15$. Yet, MT/LMOD produced more compact conformational ensembles than LowModeMD or Stochastic Search. At $\Delta E = 15$, LowModeMD gave NbConfs = 755, more than twice the output of MT/LMOD

(NbConfs = 345). This finer sampling by LowModeMD versus MT/LMOD, however, did not improve the retrieval rate of the bioactive structures.

Increasing the number of moves per rotatable bond (RotSteps) with MT/LMOD from 100 (default) to 400 augmented %BioConf_Rep from 92% to 97%. This effect was even more pronounced with the Flexible and Macrocycle sets (below). Incidentally, MT/LMOD with GB (default) performs much better (%BioConf_Rep = 89%) than when run with a distance-dependent dielectric Diel (%BioConf_Rep = 73%), consonant with Diel yielding a lower NbConf value (55) than GB (NbConf = 101). That is consistent with the results obtained with MOE, and other compound sets.

In sum, for a compound in the flexibility range of the Drug-like set, it is highly likely that a conformer close to its bioactive structure can be generated by force field based conformational sampling, in agreement with previous studies.[22,24,30,31,33,46] If a conformer within 2.0 Å is sufficient, then virtually all search methods reproduce 100% of the bioactive structure. However, a deviation of 2.0 Å for small compounds is large and arguably frequently too vague to be operational in drug design. Since the computed conformers are energy minimized, and the sampling is clearly not a limiting factor with the Drug-like compounds, the implication is that the reference bioactive structures also tend to be geometrically close (within 1 Å) to an energy minimum. The searches perform clearly better with GB, consistent with this solvation model being the default in MacroModel. It is unclear why that is not also the case in MOE, and changing the default settings from Diel to GB in MOE should be considered. For the Drug-like compounds, the best %BioConf_Rep values were achieved with $\Delta E = 15$, while Stochastic Search, LowModeMD, MT/LMOD and MT/LLMOD yielded largely equivalent values of %BioConf_Rep from 94% to 97% within 1 Å.

3.4. Reproduction of bioactive structures with the flexible set of compounds

Compounds larger and more flexible than those commonly perceived as drug-like are also relevant for pharmacology and drug
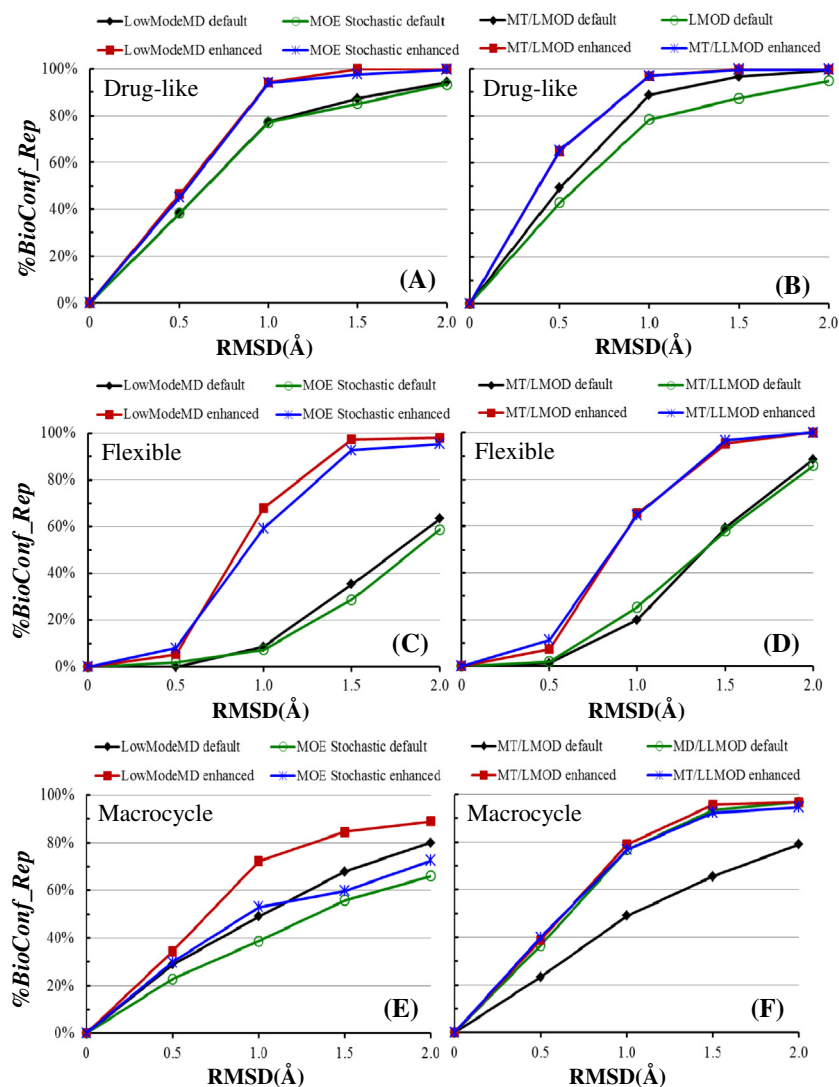
Figure 5. Cumulative percentages of reproduced bioactive X-ray structures by a computed conformer (*%BioConf_Rep*) within 0.5, 1.0, 1.5 and 2.0 Å, for the three compound sets and selected conformational sampling protocols. Results for the Drug-like set are in panels A and B, for the Flexible set in panels C and D, and for the Macrocycles in panels E and F. Panels A, C and E show the protocols with the MOE methods, that is LowModeMD at default settings (black diamonds), enhanced LowModeMD (red squares), Stochastic Search at default settings (green circles), and enhanced Stochastic Search (blue stars). Panels B, D and F show the protocols from MacroModel, that is MT/LMOD at default settings (black diamonds), enhanced MT/LMOD (red squares), MT/LLMOD at default settings (green circles), enhanced MT/LLMOD (blue stars), LMOD at default settings (green circles, panel B), and default MD/LLMOD (green circles, panel F). Parameters for the default settings are in Table 1, and in Table 6 for the enhanced protocols.

discovery (see Section 1). Thus, we curated a set of 50 chemically diverse Flexible ligands (examples in Fig. 2) with good quality and publicly available bioactive X-ray structures, including various protein classes. Their number of nonterminal rotatable bonds range from 12 to 17 (Fig. 4). We use the shorthand 'Flexible compounds' to refer to compounds of the Flexible set.

Table 3 summarizes the performance of the computational searches regarding *%BioConf_Rep* and NbConfs on the Flexible compounds. Figure 5 compares *%BioConf_Rep* results for selected protocols. The *%BioConf_Rep* values refer to those obtained at the 1.0 Å RMSD threshold unless specified otherwise. They are lower than their counterpart with the Drug-like compounds (Table 2). That is expected since it is more difficult to find a particular conformer in the larger conformational space of the Flexible compounds. Indeed, the RMSD between a bioactive structure and its closest computed conformer increases with the number of rotatable bonds (Fig. 6). *%BioConf_Rep* is markedly degraded relative to the Drug-like compounds with LMOD and, to a lesser degree, with Stochastic Search. The best *%BioConf_Rep* values (1.0 Å threshold) were 70% (LowModeMD), 65% (MT/LMOD), 65% (MT/LLMOD). Importantly

from a methodological point of view, the Flexible set revealed differences in the performances of the search algorithms, which were otherwise not expressed with the less demanding Drug-like compounds. Regarding MacroModel, this section concentrates on the results obtained with OPLS2005, since the OPLS2.0 and MMFFs potentials yielded similar results (Table 3).

With the default settings, all methods perform poorly with the Flexible compounds, with *%BioConf_Rep* values of 7% (LMOD and Stochastic Search), 9% (LowModeMD), 10% (LLMOD), 20% (MT/LMOD), and 25% (MT/LLMOD). The better performances of MT/LMOD and MT/LLMOD over Stochastic Search and LowModeMD reflect the use of *GB* in the MacroModel default settings. Indeed, when replacing *Diel* by *GB*, keeping the other default MOE options, Stochastic Search and LowModeMD perform dramatically better, with *%BioConf_Rep* rising from 7% to 41% (Stochastic Search) and from 9% to 47% (LowModeMD). LowModeMD reproduced more Flexible bioactive structures than Stochastic Search, a trend maintained with further enhanced settings. Thus, the Flexible set stresses the need to perform the searches with *GB* even more acutely than the Drug-like set. It is clearly worth incurring the additional
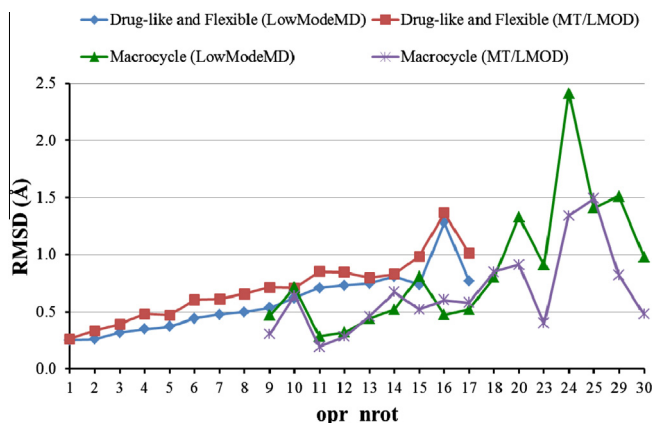
Figure 6. Influence of the number of Oprea rotatable bonds per compound (opr_nrot, *X*-axis) on the average RMSD (Å) between the best matching computational conformer and the corresponding bioactive X-ray structure. The data for the Drug-like and Flexible compounds were combined (blue diamonds and red squares) since these compounds differ only by their flexibility (opr_nrot) and there is continuity between the less flexible Drug-like compounds and the Flexible set. The data for the Macrocycle set are plotted separately, since the overall flexibility of the Macrocycle compounds is affected by their ring closure constraint. The data are shown for conformational ensembles generated by enhanced LowModeMD (blue diamonds for Drug-like and Flexible sets; green triangles for the Macrocycles), and by enhanced MT/LMOD (red squares for Drug-like and Flexible sets; magenta stars for the Macrocycles). See Table 6 for the definition of enhanced LowModeMD and enhanced MT/LMOD. For a same opr_nrot value, the RMSD between the bioactive structure and the closest computed conformer tends to be lower for the Macrocycles than for the Drug-like and Flexible compounds. Some larger values of opr_nrot correspond to small numbers of compounds (e.g. a single compound at opr_nrot = 30), so the corresponding RMSDs are only indicative and not statistically robust.

computational demand of using *GB*, instead of accepting the default faster calculations with *Diel* in MOE.

Even with *GB*, the protocols with the default energy windows (7 kcal/mol in MOE, 5 kcal/mol in MacroModel) gave *%Bio-Conf_Rep* ⩽ 50%. Increasing Δ*E* had more impact on improving *%BioConf_Rep* with the Flexible than the Drug-like set. Widening Δ*E* to 15 increased *%BioConf_Rep* by around 20% (18% with Stochastic search, 20% with MT/LMOD, and 21% with LowModeMD). Indeed, increasing Δ*E* from 7 to 15 (with *GB*) yielded NbConfs values ∼3 times larger with the MOE protocols. In addition to retain conformers of higher energy, an increased Δ*E* may also facilitate crossing of the high energy regions separating lower energy conformers. The higher energy window needed to reproduce bioactive structures of the Flexible set is reminiscent of suggestions that the strain energy of ligands (as represented by force fields) appears to increase with the number of rotatable bonds.[21,70–72] However, broadening Δ*E* further from 15 to 20 kcal/mol only improved *%BioConf_Rep* from 68% to 70% with LowModeMD, and left *%BioConf_Rep* unchanged at 45% with MT/LMOD (Table 3). Thus, increasing Δ*E* from its default values to 15 kcal/mol markedly improves *%BioConf_Rep*, but this effects plateaus for higher values of Δ*E*, similar to previous experiences on other compound sets.[22,71] Increasing Δ*E* is a trade-off between enriching the conformational ensemble with diverse conformers which may improve *%BioConf_Rep*, and adding implausible high energy conformers. The present tests suggest that Δ*E* = 15 kcal/mol is a good compromise with Flexible compounds. The remainder of this section focuses on results obtained with Δ*E* = 15 kcal/mol.

With LowModeMD (*GB* and Δ*E* = 15) over two thirds (68%) of the bioactive structures of the Flexible compounds were reproduced within 1 Å, while Stochastic Search with the same parameters performed notably less well (*%BioConf_Rep* = 59%). For MT/LMOD, increasing Max-Iteration from 10,000 to 20,000 did not improve *%BioConf_Rep*. Instead, the results were strongly influenced
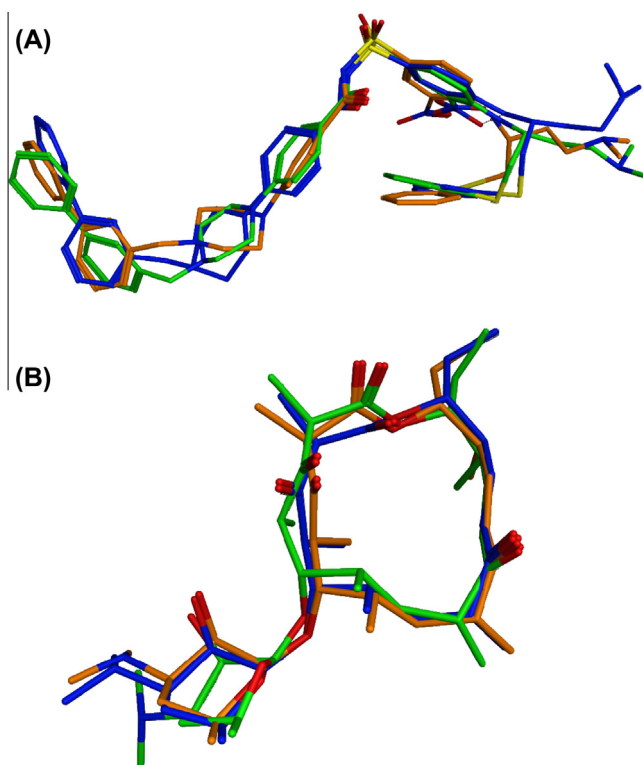

Figure 7. Examples of computed conformers superimposed after best-fit on their corresponding X-ray bioactive structure (green carbons). Panel A shows a protein-protein interaction inhibitor (Flexible set, 17 rotatable bonds) from PDB entry 3INQ, and panel B shows a macrocycle (Macrocycle set, 18 rotatable bonds) from PDB entry 2C7X. The conformer which was generated by enhanced LowModeMD and was closest (RMSD ∼1 Å) to the bioactive X-ray structure is shown with blue carbons. The conformers which was generated by enhanced MT/LMOD and was closest (RMSD ⩽ 1 Å) to the bioactive X-ray structure is shown with orange carbons. These overlays illustrate how the enhanced search protocols described in the main text and Table 6 can generate conformers close to the bioactive X-ray structure, for the Flexible and Macrocycle compounds. See Tables 3–5 for statistics summarising the reproduction of the bioactive structures for the Flexible and Macrocycle sets.

by the number of search steps per rotatable bond (RotSteps). With the default RotSteps = 100, MT/LMOD (*GB*, Duplicate RMS = 0.25 Å, Max-Iterations = 10,000) gave *%BioConf_Rep* = 45%. Increasing RotSteps to 200 and 400 dramatically increased *%BioConf_Rep* to 55% and 65%, respectively. A marked increase of *%BioConf_Rep* when augmenting RotSteps was also observed with MT/LLMOD (Table 3). At the default RotSteps = 100, MT/LLMOD performed better (*%BioConf_Rep* = 53%) than MT/LMOD (*%BioConf_Rep* = 45%). This apparent advantage, however, disappeared when RotSteps was increased to 400. Thus, increasing RotSteps had more impact than selecting between MT/LMOD or MT/LLMOD. Another protocol which involves LLMOD moves is MD/LLMOD, which was specifically developed for macrocycles, but was also tested on the Flexible set. At default settings, MD/LLMOD yielded a respectable *%BioConf_Rep* = 50% (RMSD ⩽ 1 Å). However, the current implementation of MD/LLMOD does not offer the option to increase RotSteps, which, in view of the present results, could be worth implementing. The quality of the fit between computed conformers and bioactive X-ray structure for a Flexible compound is illustrated in Figure 7A.

Increasing RotSteps two fold multiplies NbConfs by almost 2, consistent with the impact of this parameter. Doubling RotSteps approximately doubled the compute time, so exploring RotSteps values above 400 became prohibitive on the full Flexible set. If handling only a few compounds, however, one might increase RotSteps even further. Thus, RotSteps is a key parameter to improve the performance of low-mode methods in MacroModel.

With RotSteps = 400, MT/LMOD (%BioConf_Rep = 65%, RMSD ⩽ 1 Å) and MT/LLMOD (%BioConf_Rep = 65%) performed almost as well as MOE LowModeMD (%BioConf_Rep = 68%). Overall, LowModeMD gave the highest %BioConf_Rep value with the Flexible set (1.0 and 1.5 Å thresholds), suggesting that its distinctive attributes (recalculation and use of the low-frequency modes at every iteration) offer advantages.

LowModeMD (GB and ΔE = 15) produced more conformers (NbConfs = 5448) than MT/LMOD (NbConfs = 4452, RotSteps = 400) and Stochastic Search (NbConfs = 3986). The ranking of these NbConfs values reflect that of the associated %BioConf_Rep values. Thus, a finer sampling of the conformational space gives a greater chance to obtain a close representative of the bioactive binding mode. This was a systematic trend across the range of opr_nrot values when comparing LowModeMD to MT/LMOD for the combined Drug-like and Flexible sets (Fig. 6). Although LowModeMD and Stochastic Search performed equally well with the Drug-like set, that was no longer the case with the Flexible set, and LowModeMD emerged as the method of choice with MOE. With MacroModel, the Flexible set magnified the benefits of MT/LMOD and MT/LLMOD over their counterparts without torsional moves; including torsional sampling helps.

As expected, %BioConf_Rep increases as one relaxes the RMSD threshold defining reproduction of the bioactive structure. It was very encouraging to find that, for RMSD ⩽ 1.5 Å, %BioConf_Rep = 97% with LowModeMD (ΔE = 15), since reproducing a bioactive structure within 1.5 Å is a fair performance for large Flexible compounds. A similar performance was obtained with MT/LMOD (RotSteps = 400), yielding %BioConf_Rep = 95% for RMSD ⩽ 1.5 Å. When relaxing the RMSD threshold further to 2.0 Å, most protocols at ΔE = 15 gave %BioConf_Rep ⩾ 95%, except LMOD. Thus, even a lesser sampling (as with MT/LMOD at RotSteps = 100) generally affords a low-resolution representation (RMSD ⩽ 2.0 Å) of the bioactive structures of the Flexible compounds.

Overall, the results show that reproducing the bioactive structures of large Flexible compounds is a realistic prospect with modern protocols and computational resources. When approaching such tasks, the choice of sampling method and parameters has more impact than with simpler compounds, and clearly benefits from adjustments to the default settings. Our tests stress the benefits of GB solvation combined with energy windows more permissive than the default settings, typically ΔE = 15 kcal/mol. The spread of performances across the spectrum of low-mode based approaches highlights the value of successive algorithmic developments. Indeed, the recent efficient algorithm implemented in LowModeMD performs comparatively well. Also, the MacroModel methods show that combining low-mode and torsional moves performs better than pure low-mode moves. So, it may be worth inserting some torsional moves along a LowModeMD search.

3.5. Reproduction of bioactive structures with the macrocycle compounds with MOE and MacroModel

Renewed attention has been paid to macrocycles in recent years, from the medicinal and computational chemistry points of view.[27,34,47,51] This was part of the impetus for the development of the LowModeMD method.[34] The generic MacroModel protocols applied to Macrocycles are summarized in Table 4. Since some parameters tunable with MD/LLMOD are distinct, the corresponding results are summarized in Table 5 and the next section. The Macrocycle set contains 30 carefully assembled compounds (see Section 2). Examples of investigated Macrocycles are shown on Figure 3. Including the cyclic moieties, the number of rotatable bonds ranges from 9 to 30 in the Macrocycle set (Fig. 4), with 10 compounds having at least 20 rotatable bonds. Considering only the

number of rotatable bonds, the Macrocycle set would represent the most flexible investigated compounds. Yet, the conformational space is curbed by the ring closure constraint in the Macrocycles. The following analysis concentrates on %BioConf_Rep obtained at RMSD ⩽ 1 Å unless specified otherwise.

Some of the trends already highlighted with the Drug-like and Flexible sets were confirmed with the Macrocycles. The MOE protocols performed again clearly better with GB than with Diel (Table 4). Increasing the allowed energy window from default values to ΔE = 15 markedly improved %BioConf_Rep, but no further improvement was observed when increasing ΔE from 15 to 20 kcal/mol. When widening ΔE from 7 to 15 (with GB), NbConfs increased dramatically, 6.5 and 8.9 times with Stochastic Search and LowModeMD, respectively. However, a further broadening of ΔE from 15 to 20 only increased NbConfs 1.4 times with LowModeMD, illustrating again that the widening of ΔE is only operational on a limited range. Consequently, the following concentrates on results obtained at ΔE = 15 kcal/mol.

LowModeMD (GB and ΔE = 15) reproduced 72% of the Macrocycle bioactive structures, similar to the result obtained with the Flexible set (68%). With the same parameters, Stochastic Search only achieved %BioConf_Rep = 53%, stressing the benefits of LowModeMD when exploring macrocycles with MOE. However, at default settings LowModeMD reproduced less than half (49%) of the bioactive structures. Considering the challenging synthetic efforts usually incurred by macrocycles,[47,51] it is well worth enhancing the computational settings towards more accurate and predictive models.

The MacroModel protocols matched the LowModeMD performance, with search parameters enhanced above the default values (Table 4). At default settings MT/LMOD and LMOD gave %BioConf_Rep values of 49% and 40%, respectively. MT/LMOD performed again better than LMOD. The best performance of MT/LMOD gave %BioConf_Rep = 79% (GB, Duplicate RMS = 0.25, OPLS2005, MaxIterations = 10,000, RotSteps = 400). With the same parameters, MT/LLMOD performed similarly, with %BioConf_Rep = 77%. As with the Flexible set, increasing RotSteps led to notably increased %BioConf_Rep and NbConfs values, that is %BioConf_Rep improved from 64% (RotSteps = 100) to %BioConf_Rep = 79% (RotSteps = 400, OPLS2005) with MT/LMOD. After increasing RotSteps, MT/LMOD and MT/LLMOD performed at least as well as LowModeMD. With RotSteps = 400, NbConfs was larger (2415) with MT/LMOD than produced (1675) by LowModeMD (GB, ΔE = 15). This suggests again that LowModeMD might benefit from the insertion of torsional moves. A good fit between the bioactive X-ray structure of a macrocycle and computed conformer is illustrated in Figure 7B.

When relaxing the RMSD threshold at which %BioConf_Rep is examined, the results are even more promising with all methods (Table 4). Within RMSD ⩽ 1.5, %BioConf_Rep ranges from 84% with LowModeMD to 96% with MT/LMOD (RotSteps = 400, OPLS2005). Within RMSD ⩽ 2.0, %BioConf_Rep ranges from 89% with LowModeMD to 98% with MT/LMOD. These %BioConf_Rep values at the 2 Å threshold are somewhat lower than those with the Flexible set. Indeed, it is only with the Macrocycle set that %BioConf_Rep does not reach 100% for RMSD ⩽ 2 Å. This may be because the number of rotatable bonds extends to higher values with the Macrocycle set than with the Flexible set (Fig. 4). Yet, the same protocols generated fewer conformers per compound for the Macrocycles than for the Flexible compounds. For example, LowModeMD (ΔE = 15) gave NbConfs = 1675 for the Macrocycles and NbConfs = 5448 for the Flexible set; MT/LMOD (RotSteps = 400, OPLS2005) produced NbConfs = 2415 for the Macrocycles and NbConfs = 4452 for the Flexible set. The lower NbConfs values with the Macrocycles likely reflect the associated ring closure constraints. This is consistent with the notion that even large macrocycles have a reduced conformational space compared to

noncyclic molecules, which would reduce the entropic cost of binding to their biological targets. The ring closure constraint also may explain why, at same values of opr_nrot, the computed conformers tend to be closer to the bioactive X-ray structure with the Macrocycles than with the Flexible compounds (Fig. 6). Overall, even with highly flexible Macrocycles, modern computational sampling tools are very likely to generate a mimic of their bioactive structure. That is reinforced by the results obtained with MD/LLMOD.

3.6. Reproduction of bioactive structures of the macrocycles with MD/LLMOD

MD/LLMOD is an approach recently developed by Schrödinger specifically for macrocycles. With MD/LLMOD, an MD high-temperature simulated annealing is followed by LLMOD moves (see Section 2). The *%BioConf_Rep* values obtained with MD/LLMOD protocols are summarized in Table 5. Again, the analysis concentrates on *%BioConf_Rep* obtained at RMSD $\leqslant$ 1 Å unless specified otherwise.

The default settings reproduced 77% and 97% (RMSD $\leqslant$ 2 Å) of the bioactive conformers, which is among the best results obtained for the Macrocycle set. That is only marginally less than *%BioConf_Rep* = 79% obtained with the most thorough MT/LMOD protocol, and above *%BioConf_Rep* = 72% obtained with LowModeMD. In light of the above discussion, the good performance of MD/LLMOD is likely due to a sufficiently wide default energy window (ΔE = 10 kcal/mol). Adjusting the default parameters one at a time did not improve *%BioConf_Rep*, despite sometimes increasing NbConfs (Table 5). Replacing *GB* solvation by *Diel* markedly degraded the results, consistent with all equivalent tests. Increasing ΔE to 15 kcal/mol did not improve *%BioConf_Rep*, nor did an increase in the number of LLMOD steps, nor lowering the duplicate RMS cutoff, nor replacing OPL2005 by the newer OPLS2.0. Yet, those adjustments increased NbConfs, which may be helpful in some applications. Similarly, recalculating the eigenvectors at every search step did not increase *%BioConf_Rep* within 1 Å (73%), but increased NbConfs relative to default settings. The slight degradation of *%BioConf_Rep* when recalculating the eigenvectors at every step is intriguing. However, calculating the eigenvectors only once on the initial conformer did reduce *%BioConf_Rep* by 10%. Thus, recalculating the eigenvectors only for each new global energy minimum appears to be a judicious compromise. Notably, turning off the first MD stage degrades the results considerably (*%BioConf_Rep* = 60%), demonstrating the importance of the first simulated annealing phase. Comparison with MT/LMOD suggests that MD/LLMOD might benefit from inserted torsional moves, even if this may appear counterintuitive with cyclic

topologies. Only a small gain (*%BioConf_Rep* = 80%) was observed by combining Duplicate RMS = 0.25 Å, ΔE = 15 kcal/mol and Max-Iterations = 10,000. Overall, the present tests confirm that the MD/LLMOD default settings are well-balanced, and that this approach should prove effective for the conformational sampling of macrocycles.

3.7. Influence of the force field

Three mainstream force fields were used in the present study, MMFF, OPLS2005 and OPLS2.0. MMFF94x (default in MOE) and MMFFs (optional in MacroModel) can be regarded as both representative of MMFF. The recent OPLS2.0 is an extensive reparameterization of OPLS2005, so we consider them as different force fields. Detailed tests of force fields are complicated and involved tasks which are beyond the scope of the present work. However, it was of interest to test if different force fields would affect the general behavior of the sampling protocols, e.g. regarding NbConfs and *%BioConf_Rep*. One may consider that reproduction of bioactive X-ray structures by computed conformers provides an assessment of the underlying force field, assuming sufficient sampling. That can only be a crude test, since the bioactive structures may not coincide with an energy minimum of the ligands,[21,23,70] while the computed conformers are energy-minimized. Yet, one expects that well-resolved bioactive structures can only be consistently reproduced, or approximated, by well-balanced force fields.

This was touched upon with MT/LMOD protocols (GB, ΔE = 15, Duplicate RMS = 0.25, Max-Iterations = 10,000, RotSteps = 100) being repeated with OPLS2005, OPLS2.0 and MMFFs (Tables 2–4). With this protocol, the investigated potentials led to similar results regarding *%BioConf_Rep* values (RMSD $\leqslant$ 1 Å). With the Drug-like set (Table 2), OPLS2005, OPLS2.0 and MMFFs gave *%BioConf_Rep* = 92%, *%BioConf_Rep* = 92% and *%BioConf_Rep* = 93%, respectively. With the Flexible set (Table 3), OPLS2005, OPLS2.0 and MMFFs gave *%BioConf_Rep* = 45%, *%BioConf_Rep* = 41% and *%BioConf_Rep* = 43%, respectively. With the Macrocycle set (Table 4), OPLS2005, OPLS2.0 and MMFFs gave *%BioConf_Rep* = 64%, *%BioConf_Rep* = 72% and *%BioConf_Rep* = 64%, respectively. The better *%BioConf_Rep* obtained with OPLS2.0 and RotSteps = 100 for the Macrocycles was not confirmed with RotSteps = 400 (OPLS2005: *%BioConf_Rep* = 79%; OPLS2.0: *%BioConf_Rep* = 73%). Indeed, with MD/LLMOD applied to the Macrocycles (Table 5), *%BioConf_Rep* was also larger with OPLS2005 (77%) than with OPLS2.0 (67%). Overall, the rate of reproduction of the bioactive structures was not strongly dependent on the force fields, and was instead dominated by the extent of the sampling and the treatment of electrostatics (*Diel* vs *GB*).

In addition, OPL2005, OPLS2.0 and MMFFs generated similar NbConfs values (Tables 2–4). This suggests that the ruggedness of

Table 6
Summary of the parameters for the best-performing 'enhanced' conformational sampling protocols[a]

Software	Search method	Solvation[b]	Duplicate RMS[c] (Å)	ΔE[d]	Max-Iterations[e]	RotSteps[f]
MOE	LowModeMD	GB	0.25	15	10,000	NA[i]
MacroModel	MT/LMOD[g]	GB	0.25	15	10,000	400
	MT/LLMOD[h]	GB	0.25	15	10,000	400

[a] Combinations of methods and parameters which yielded the best overall performance in the present study. These 'enhanced' protocols require parameters augmented above the default settings. MD/LLMOD also performed well for macrocycles, but is not listed here since its default settings were found to be adequate; in addition MD/LLMOD is not adapted to Drug-like compounds, and its relevance to nonmacrocyclic Flexible compounds is unclear.
[b] *GB*: generalized Born solvation model.
[c] Root mean square deviation cutoff to remove duplicate conformers.
[d] Allowed conformational energy window (kcal/mol) for the conformers.
[e] Maximum number of search iterations.
[f] RotSteps was only applicable to the MacroModel protocols, and specifies the maximum number of moves per rotatable bond.
[g] Mixed torsional/Low-mode.
[h] Mixed torsional/Large-scale low-mode.
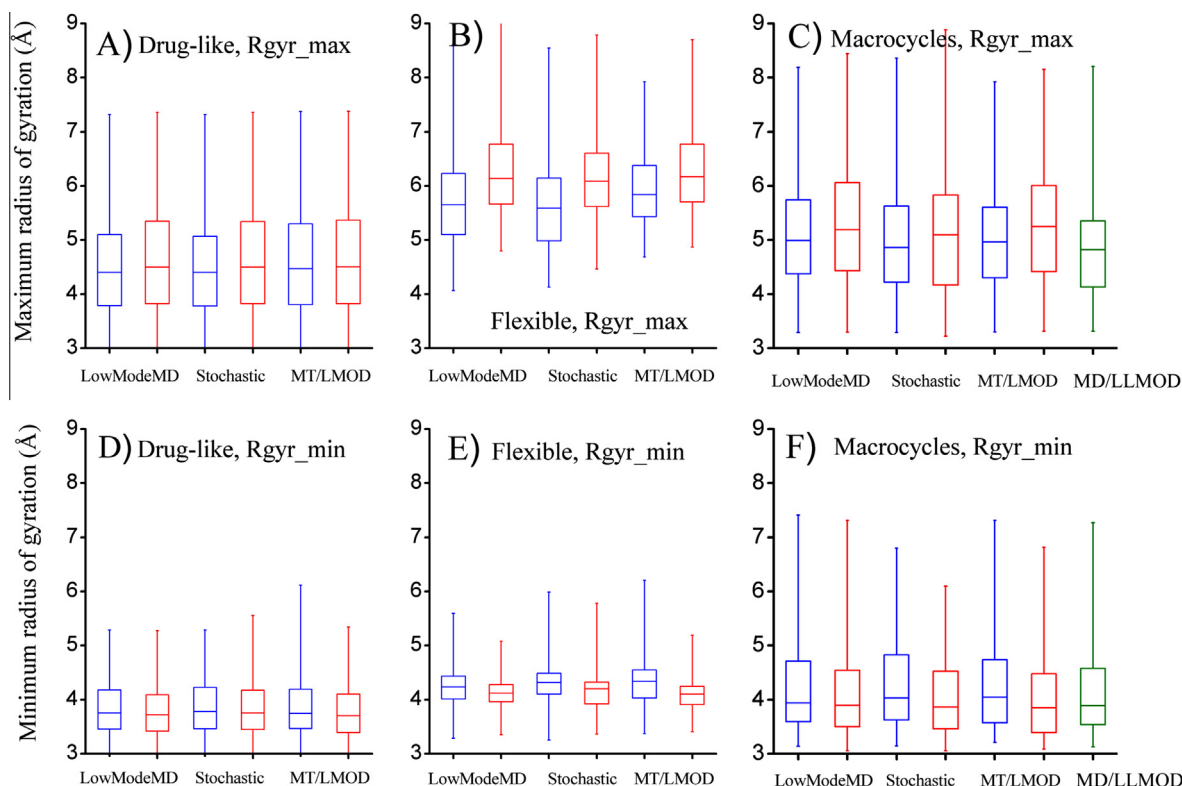[i] Not applicable.

Figure 8. Distributions of the minimum (Rgyr_min) and maximum (Rgyr_max) radius of gyration (Å) for default and enhanced protocols for compounds in the Drug-like (left-most panels), Flexible (middle panels) and Macrocycle (right-most panels) sets. Distributions of Rgyr_max are in the top panels A, B and C. Distributions of Rgyr_min are in the bottom panels D, E and F. For each compound set, the protocols are the MOE LowModeMD, the MOE Stochastic Search ('Stochastic') and the MacroModel MT/LMOD. The default MD/LLMOD protocol (green, right of panels C and F) is shown for the Macrocycle set. For LowModeMD, Stochastic Search and MT/LMOD, the default protocols are in blue, and the enhanced protocols in red. The parameters for the enhanced protocols are in Table 6; for Stochastic Search they are the same as for LowModeMD. The distributions are depicted as box-plots. Each box extends from the first to the third quartile and the horizontal bar marks the median; the 'wiskers' extend to the minimum and the maximum values.

the energy surfaces underpinned by these potentials is similar. Indeed, no potential was associated with significantly more distinct energy minima than the others. This suggests that the investigated force fields lead to similar overall conformational coverages, when assessed via NbConfs or *%BioConf_Rep*. Sections 3.8 and 3.9 provide additional characterizations of the conformational coverage.

Overall, the above results indicate that the best performing protocols in the present study are those reported in Table 6. We refer to those as 'enhanced' protocols since they involve parameter settings augmented above the default settings. These protocols rely on LowModeMD or MT/LMOD, or MT/LLMOD. MT/LMOD performed in practice as well as MT/LLMOD even for the most flexible compounds, despite MT/LLMOD scaling better with system size in theory. In addition, MT/LMOD is in principle the MacroModel method of choice for Drug-like compounds. Thus, the following focuses primarily on comparisons between enhanced LowModeMD and enhanced MT/LMOD. Enhanced MT/LMOD and enhanced LowModeMD took on average about 6 and 7 times longer to run than their default counterparts, respectively.

3.8. Conformational coverage assessed by the compactness/extendedness of the compounds

Conformational coverage refers to the extent and resolution with which a conformational model covers the conformational space.[38,67,68] An absolute characterization of the conformational coverage is difficult, but the output from different protocols may be compared in relative terms. NbConfs and *%BioConf_Rep* already gave valuable indications about the coverage (see above). Further characterization is possible by examining the range of compact-

ness/extendedness populated by the conformers. For each conformer, this was probed by its radius of gyration (Rgyr). The discussion emphasizes the Flexible and Macrocycle sets, since they are the thrust of the present study.

Figure 8 presents the distributions of minimum (Rgyr_min) and maximum (Rgyr_max) Rgyr values for conformers obtained by selected sampling protocols. The distributions at default settings (blue) are shown on the left of the corresponding distributions from the enhanced protocol (red). For MD/LLMOD with the Macrocycles (green, right of panels C and F), only the distribution at default settings is shown since altering those settings did not yield notable improvements. The distributions are represented with boxplots where the middle bar represents the median; one can compare the median values. For Rgyr_max (Fig. 8A–C) the enhanced protocols yielded distributions shifted to higher Rgyr_max values; this is particularly notable with the Flexible and Macrocycle sets. Thus, the enhanced protocols found more extended conformers than the default settings. For Rgyr_min (Fig. 8D–F) the enhanced protocols yielded distributions shifted to lower Rgyr_min values with the Flexible and Macrocycle sets. So, the enhanced protocols also found more compact conformers than the default settings. Thus, the enhanced sampling protocols (Table 6) did generate conformers with a greater range of compactness/extendedness than the default settings, yielding greater conformational coverage.

Figure 9 compares the Rgyr values of the bioactive X-ray structures (Rgyr_X-ray, green) to Rgyr_min (blue) and Rgyr_max (red) computed by selected protocols (caption of Fig. 9). With these protocols, Rgyr_X-ray is well within the interval between Rgyr_min and Rgyr_max for most compounds. That was also observed with
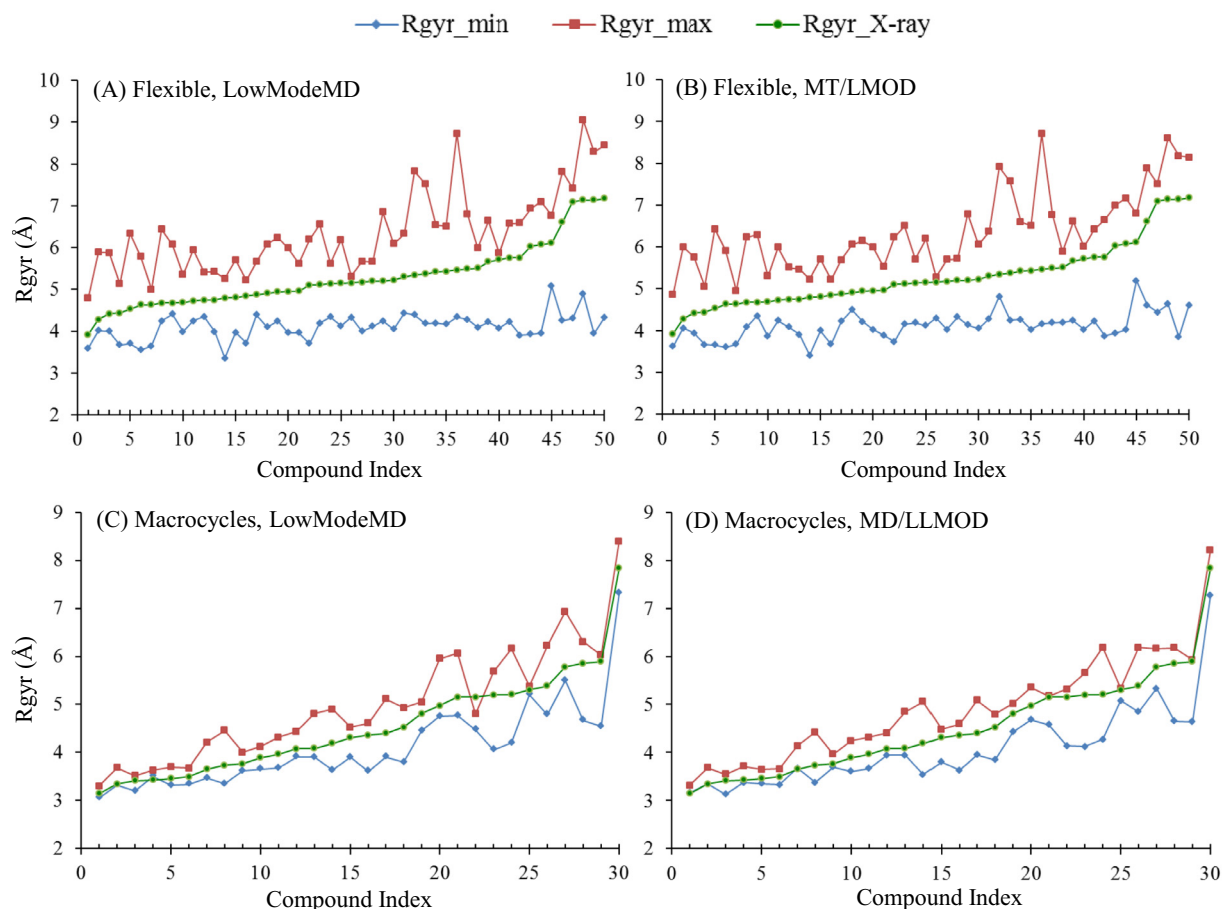
Figure 9. Minimum (Rgyr_min, blue diamonds) and Maximum (Rgyr_max, red squares) values of the radius of gyration (Å) from selected computational protocols are shown alongside Rgyr_X-ray for the corresponding bioactive X-ray structures (green circles). Panels A and B: compounds of the Flexible set; Panels C and D: compounds of the Macrocycle set. Compounds are sorted individually along the X-axis by increasing Rgyr_X-ray values. The Rgyr_X-ray values lie between the computed Rgyr_min and Rgyr_max values for the vast majority of the compounds. The computed Rgyr values were from enhanced protocols, with parameters reported in Table 6. Panel A: enhanced LowModeMD and Flexible compounds; panel B: enhanced MT/LMOD and Flexible compounds; panel C: enhanced LowModeMD and Macrocycle compounds; panel D: default MD/LLMOD (default settings) for the Macrocycles.

the Drug-like compounds (not shown). Thus, the experimental range of extendedness is covered by the enhanced protocols and MD/LLMOD. A finer description of the conformational coverage can be obtained via the 3D pharmacophores visited by the conformational ensembles.

3.9. Coverage of the 3D pharmacophoric space

In addition to the range of compound compactness/extendedness (previous section), a finer-grained view of the coverage of the conformational space can be obtained by the number of 3D pharmacophores visited by a conformational ensemble.[22,24,27,30] It estimates the diversity of the generated conformers while having some relevance for molecular recognition. This was quantified by counting the number of visited 3D three-point pharmacophores per (selected) sampling protocol and per compound set. For a given conformational ensemble, each visited pharmacophore was counted only once. The 3D three-point pharmacophores were defined with the Phase pharmacophoric features, coded with Canvas fingerprint (see Section 2). The greater the number of visited pharmacophores the greater the conformational coverage, and the greater the diversity of the generated conformers.

The number of pharmacophores visited by selected protocols for the Drug-like, Flexible and Macrocycle sets are shown in Figure 10. Each panel displays the count of pharmacophores visited

by LowModeMD, Stochastic Search and MT/LMOD at default settings (blue bars), and with enhanced search parameters (red bars); the parameters defining the enhanced searches are in Table 6. In Figure 10, the dark blue shade represents the count of visited pharmacophores common across the protocols at default settings, while the dark red shade shows the number of pharmacophores common across the enhanced protocols. The lighter shades display the number of pharmacophores which are not in common. The two bars shown for MD/LLMOD in Figure 10C both represent the default settings of MD/LLMOD, compared either to the default of other protocols (blue) or to the enhanced other protocols (red).

Since, for a given protocol, the number of visited pharmacophores was aggregated across all the compounds of a set (Drug-like, Flexible or Macrocycles), this number depends on the number of compounds in the set. Thus, rigorous comparisons can only be made within a compound set. Yet, one notes that the number of visited pharmacophores is smaller for the Drug-like set, despite this set containing more compounds (253) than the Flexible (50) and Macrocycle (30) sets. This is because the larger compounds in the Flexible and Macrocycle are more feature rich. Across a same compound set, most pharmacophores were found in common by different sampling protocols (dark blue or dark red shade of the bars in Fig. 10). That implies that largely equivalent regions of the conformational space were covered by the tested protocols. In this context, it is interesting to remember that different force

fields were used by MOE (MMFF94x) and MacroModel (OPLS2005), and it was initially not clear whether these different energy models would promote divergent explorations of the conformational space. There is no indication that large areas of the conformational space were explored by some protocol but not the others. This large overlap in conformational coverage is reassuring, since it suggests that a good degree of convergence was reached by the searches, even for the Flexible and Macrocycle compounds.

For each compound set, the enhanced protocols clearly visited more pharmacophores than the default protocols. For example,
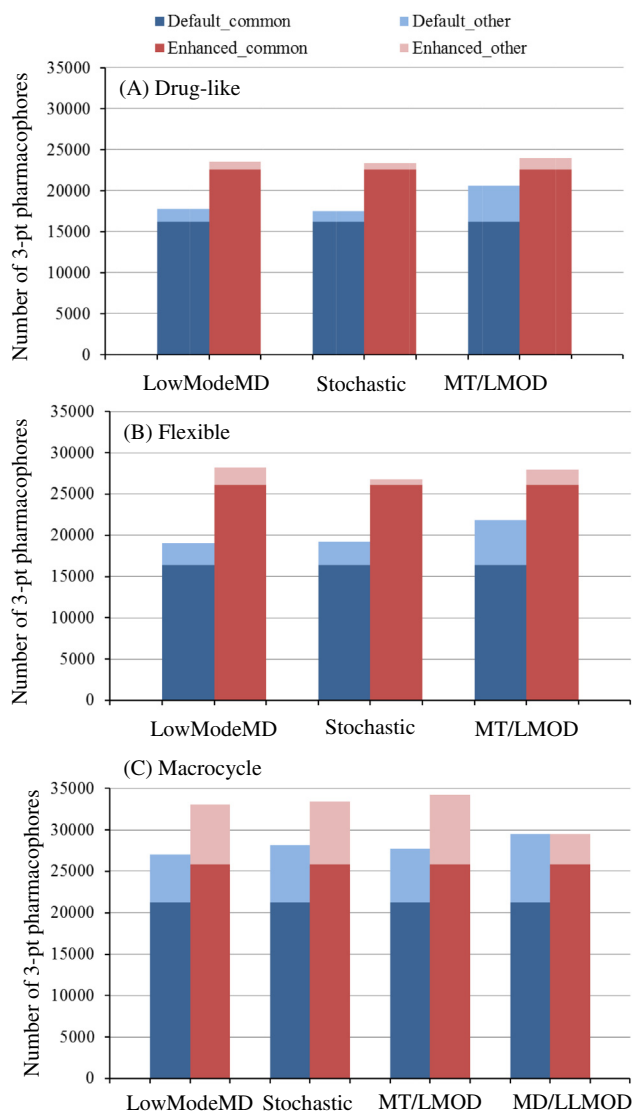

Figure 10. Conformational diversity estimated with the number of visited 3-point 3D pharmacophores (Y-axis) for selected search protocols, with (A) the Drug-like set, (B) the Flexible set, and (C) the Macrocycle set. Each method is noted on the X-axis underneath the corresponding bar charts. The methods are LowModeMD, Stochastic Search ('Stochastic'), MT/LMOD and MD/LLMOD (Schrödinger protocol specialized for Macrocycles). The blue bars represent the protocols at default settings (Table 1) and the red bars are for the corresponding enhanced protocols (Table 6, same parameters for Stochastic Search as LowModeMD). The dark blue part of every blue bar is the number of visited pharmacophores common to all default protocols, and the light blue represents the number of other pharmacophores (not in the intersection between the default protocols). The dark red part of every red bar is the number of visited pharmacophores common to all enhanced protocols, and the light red part is the number of other pharmacophores (not in the intersection between the enhanced protocols). The two bars for MD/LLMOD were obtained with the same default protocol, but present the number of pharmacophores in common with the other default protocols (blue bar) or in common with the other enhanced protocols (red bar).

with the aggregated Flexible compound set (Fig. 10B), enhanced LowModeMD generated 1.5 times more pharmacophores (28,185) than its default counterpart (19,021). That is somewhat more than the 26,754 pharmacophores produced by enhanced Stochastic Search, confirming that LowModeMD is the method of choice for Flexible compounds in MOE. Notably, enhanced MT/LMOD visited 28,000 pharmacophores, matching LowModeMD.

Enhanced MT/LMOD also performed well with the Macrocycles (Fig. 10C), since it yielded the largest number of 3D-pharmacophores (34,283), above enhanced Stochastic Search (33,403) or enhanced LowModeMD (33,098), or MD/LLMOD at default settings (29,524). Since only very limited improvements to the performance of MD/LLMOD were obtained by manipulating its parameters (Section 3.6), no enhanced variant of MD/LLMOD is reported in Figure 10. Yet, the red bar for MD/LLMOD shows that most pharmacophores visited by the *default* MD/LLMOD with the Macrocycles were in common with those sampled by the *enhanced* protocols with the other methods. Thus, the conformational coverage afforded by default MD/LLMOD is a reasonable compromise.

3.10. Consistency in finding the global energy minimum

The global minimum of the conformational energy surface plays a special role in conformational analysis since it allows an anchoring of the energy scale, and is in principle necessary to estimate the conformer populations.[22,38,69] In addition, it provides an important test of convergence for stochastic search methods which explore the energy surface while being directed to low-energy conformers by energy minimization. There is no guarantee that a stochastic search will find all the minima. A converged search would find all the minima at least once. Thus, a (simplified) test of convergence examines how frequently the global energy minimum is found by independent runs using the same search protocol. That is also another test of coverage.

To use the global energy minimum as test of convergence, this reference conformer needs to be identified in the first place, for a given energy model. This can only be done empirically for large flexible compounds, since they are not amenable to a systematic search. The identification of the global energy minimum per compound and per energy model is described in Section 2. Briefly, the output of as many search runs as possible were aggregated for a given energy model (GB with MMFF94× for MOE, or GB with OPLS2005 for MacroModel). This aggregation collated the conformational ensembles of (i) 12 MOE runs and 36 MacroModel runs for the Drug-like compounds, (ii) 15 MOE runs and 39 MacroModel runs for the Flexible compounds, and (iii) 15 MOE runs and 24 MacroModel runs for the Macrocycle compounds. The aggregation of all these conformers makes it highly likely that they contain the global energy minimum for a compound and energy model.

The identified global energy minima were then used to test how frequently they were found by individual runs of selected protocols (Table 7). The percent of compounds for which a run found the global energy minimum is called %GlobMin_found. The global energy minimum was considered found if the run produced a conformer close enough in energy (within 0.5 kcal/mol) and structure (within 0.5 Å). Of course, %GlobMin_found is not directly comparable to %BioConfRep within 0.5 Å since, contrary to the global minimum, many bioactive structures are not within 0.5 Å of an energy minimum. We concentrate on the results obtained with the enhanced search protocols (Table 6).

For the Drug-like compounds, there was excellent consistency for %GlobMin_found across the three runs of a same protocol (Table 7). Enhanced LowModeMD, enhanced MT/LMOD and enhanced MT/LMOD found the global energy minimum for ⩾97% of the Drug-like compounds. This signals excellent convergence for those protocols with Drug-like compounds. It echoes the high likelihood

Table 7
Frequency of location of the global energy minimum for selected search protocols[a]

Compound set	%GlobMin_found[b] (%)	Search method	Run	Force field	Duplicate RMS (Å)[c]	ΔE[d]	Max-Iterations[e]	RotSteps[f]
Drug-like	98	LowModeMD[g]	1	MMFF94x	0.25	15	10,000	NA
	98		2					
	97		3					
	96	Stochastic Search[g]	1	MMFF94x	0.25	15	10,000	NA
	95		2					
	93		3					
	90	MT/LMOD[h]	1	OPLS2005	0.50	5	1000	100
	91		2					
	92		3					
	94	MT/LMOD[h]	1	OPLS2005	0.25	15	10,000	100
	94		2					
	94		3					
	98	MT/LMOD[h]	1	OPLS2005	0.25	15	10,000	400
	97		2					
	97		3					
	97	MT/LLMOD[i]	1	OPLS2005	0.25	15	10,000	400
	97		2					
	97		3					
Flexible	70	LowModeMD[g]	1	MMFF94x	0.25	15	10,000	NA
	66		2					
	66		3					
	52	Stochastic Search[g]	1	MMFF94x	0.25	15	10,000	NA
	42		2					
	56		3					
	42	MT/LMOD[h]	1	OPLS2005	0.50	5	1000	100
	30		2					
	42		3					
	44	MT/LMOD[h]	1	OPLS2005	0.25	15	10,000	100
	32		2					
	44		3					
	64	MT/LMOD[h]	1	OPLS2005	0.25	15	10,000	400
	64		2					
	74		3					
	76	MT/LLMOD[i]	1	OPLS2005	0.25	15	10,000	400
	68		2					
	78		3					
Macrocycles	57	LowModeMD[g]	1	MMFF94x	0.25	15	10,000	NA
	53		2					
	57		3					
	47	Stochastic Search[g]	1	MMFF94x	0.25	15	10,000	NA
	40		2					
	53		3					
	43	MT/LMOD[h]	1	OPLS2005	0.50	5	1000	100
	33		2					
	40		3					
	40	MT/LMOD[h]	1	OPLS2005	0.25	15	10,000	100
	53		2					
	40		3					
	70	MT/LMOD[h]	1	OPLS2005	0.25	15	10,000	400
	67		2					
	60		3					
	60	MT/LLMOD[i]	1	OPLS2005	0.25	15	10,000	400
	67		2					
	70		3					

[a] The selected protocols are defined by the parameters listed in the Table; all these protocols were run with *GB*.
[b] *%GlobMin_found* is the percent of compounds for which the global energy minimum was located by a search run; see main text for the criteria adopted to consider that the global energy minimum was located. *%GlobMin_found* is reported for three individual search runs, for a given protocol.
[c] Root mean square deviation cutoff (Å) to remove duplicate conformers.
[d] Allowed relative conformational energy window (kcal/mol) for the conformers.
[e] Maximum number of search iterations.
[f] RotSteps is the maximum number of moves per rotatable bond.
[g] LowModeMD and Stochastic Search are methods available in MOE.
[h] Mixed torsional/Low-mode.
[i] Mixed torsional/Large-scale low-mode.

of reproduction of the bioactive X-ray structures within 1 Å by the same protocols (Table 2). It suggests that the search per se is essentially complete for compounds in the flexibility range of the Drug-like set.

For the Flexible and Macrocycle compounds, *%GlobMin_found* varied more across runs than with the Drug-like compounds

(Table 7), as expected when the search space expands due to a greater number of degrees of freedom. Thus, convergence remains a concern when the number of rotatable bonds is in the range covered by the Flexible and Macrocycle searches. So, when a thorough exploration of conformers is required for such compounds, it is advisable to collate the outputs from several independent searches.

The results are nevertheless encouraging, since each run for the enhanced protocols found the global energy minimum for the majority of the compounds. With the Flexible set, enhanced LowModeMD, enhanced MT/LLMOD and enhanced MT/LMOD found the global energy minimum for at least 66%, 68% and 64% of the compound, respectively (Table 7). Enhanced Stochastic Search struggled (42% ⩽ %GlobMin_found ⩽ 56%). For the Macrocycle set, %GlobMin_found was lower than with the Flexible set, but still respectable. For the Macrocycles, the best performance was achieved by enhanced MT/LMOD and enhanced MT/LLMOD, both with %GlobMin_found ⩾ 60% for every run. Enhanced LowModeMD performed less well in this experiment (%GlobMin_found ⩾ 53%), but still better than enhanced Stochastic Search (40% ⩽ %GlobMin_found ⩽ 53%).

Overall, the %GlobMin_found data indicate that the conformational sampling of compounds with 12 ⩽ opr_nrot ⩽ 30 with mainstream search techniques is not intractable and not as daunting as sometimes feared. With such molecules, the interest would likely focus on a small number of compounds of special interest, allowing to perform several searches from different starting points, which together are very likely to cover most of the conformational space. However, one needs to keep in mind that the present results were obtained with chiral centers constrained to remain as in the bioactive structures. Thus, experimental data giving information about the configuration of these centers should of course be regarded as precious.

4. Conclusions

The present work addressed the conformational sampling of three types of molecules, represented by curated sets of Drug-like, Flexible and Macrocycle compounds. The main objective was to assess mainstream conformational search tools for compounds larger and more flexible than conventionally Drug-like molecules. The search protocols were evaluated and compared with respect to (i) the average number of conformers generated per compound, (ii) their ability to reproduce a ligand bioactive X-ray structure, (iii) their propensity to find the global energy minimum, (iv) the degree of compactness/extendedness of the generated conformers (Rgyr distributions), and (v) the conformational coverage/diversity measured by the number of visited 3D pharmacophores. The performance obtained with the Flexible and Macrocycle molecules was put in perspective by comparison with the Drug-like compounds.

The investigated search methods concentrated on variants of low-mode based algorithms, widely accessible via the MOE and MacroModel softwares. All MacroModel generic low-mode variants were investigated, alongside the MD/LLMOD approach developed specifically for Macrocycles, and the recent LowModeMD algorithm from MOE. The MOE Stochastic Search, which does not rely on low-mode moves, was included for comparison. The methods were first compared at their default settings, and after adjusting important search parameters including the energy window (ΔE), the deviation cutoff for removal of duplicate conformers, the maximum total number of iterations, and the number of moves per rotatable bond when applicable. This was combined with various energy models, testing the treatment of electrostatics (*Diel* versus *GB*) and three common force fields (MMFF, OPLS2005, OPLS2.0). For most search protocols, three independent runs were performed to assess how they were affected by the stochastic element. The present study may have compiled the most extensive investigation of low-mode based search protocols to date.

Importantly, the performance of the search protocols was not dominated by variation due to their stochastic nature, since independent runs consistently returned similar NbConfs, %BioConf_Rep and %GlobMin_found values. Also, NbConfs and %BioConf_Rep were

essentially insensitive to the force fields, which seem to underpin energy surfaces of similar ruggedness. However, the results were much more sensitive to the treatment of solvation. Compared to a distance-dependent dielectric, the use of a generalized Born (*GB*) model consistently yielded more conformers and reproduced more bioactive X-ray structures. Thus, when using MOE, it is strongly recommended to select the generalized Born option, instead of the distance-dependent dielectric. Since the LowModeMD and Stochastic Search in MOE are largely intended for the extensive sampling of compounds of particular interest, setting *GB* as the default would be suitable for these methods.

Increasing the energy window above the default to 15 kcal/mol clearly improved the output of LowModeMD and Stochastic Search with the Flexible and Macrocycle compounds, yielding better %BioConf_Rep values, broader Rgyr distributions, and a greater number of visited 3D pharmacophores. With the Drug-like set, increasing ΔE only had a marginal favorable effect, and LowModeMD and Stochastic Search performed equally well for those compounds. The benefits of LowModeMD over Stochastic Search emerged when applied to the Flexible and Macrocycle sets, for which LowModeMD generated larger conformational ensembles, more likely to contain a representative of the bioactive structure. LowModeMD also located the global energy minimum more frequently than Stochastic Search. So LowModeMD with *GB* and ΔE = 15 kcal/mol emerged as the protocol of choice for thorough conformational sampling in MOE.

The quality of the results obtained with LowModeMD in MOE was matched by the best low-mode based protocols in MacroModel. Combining torsional and low-mode moves was beneficial, and MT/LMOD or MT/LLMOD performed best with MacroModel, supporting the choice of MT/LMOD as the default method in Macro-Model. The performance of MT/LMOD also benefited from adjustments to the default parameters, including increasing ΔE to 15 kcal/mol, augmenting the maximum number of iterations to 10,000, while keeping more conformers (Duplicate RMS = 0.25 Å). In addition, augmenting the number of moves per rotatable bond from 100 (default) to 400 yielded marked improvements. When performed with such enhanced parameters, MT/LMOD and MT/LLMOD performed comparatively well, for example, versus %BioConf_Rep and %GlobMin_found values. This suggests that LowModeMD and MD/LLMOD might benefit from the insertion of torsional moves.

The main search options of MD/LLMOD, recently developed specifically for macrocycles, were also investigated. Its default settings performed well and matched enhanced LowModeMD regarding the reproduction of the Macrocycle bioactive X-ray structures. This is consistent with the default energy window of MD/LLMOD being larger (10 kcal/mol) than in other default settings. The initial phase of MD-based simulated annealing was found to be essential to the success of MD/LLMOD. Calculating the eigenvectors only on the initial conformer degraded the %BioConf_Rep values, although recalculating the eigenvectors at every search step did not improve %BioConf_Rep. This confirms that recalculating the eigenvectors at every new global energy minimum (default) is an adequate compromise. However, MD/LLMOD fared less well with non-macrocyclic Flexible compounds, for which LowModeMD and MT/LMOD performed significantly better.

The majority of the bioactive X-ray structures were reproduced within 1 Å across all compound sets by the enhanced search protocols, but this performance degrades as the compounds become more flexible. The vast majority of the Flexible and Macrocycle bioactive structures were reproduced within 1.5 or 2.0 Å, a very encouraging outcome. Indeed, the bioactive X-ray structures were essentially contained in the range of Rgyr values (extendedness) explored by the computed conformers. The global energy minimum was virtually always found with the Drug-like compounds.

Lower, but still respectable, *%GlobMin_found* values were obtained for the Flexible and Macrocycle sets. Thus, the search convergence remains a concern for the more flexible compounds, but it can be addressed in practice by collating the outputs of independent search runs.

In sum, the present study confirms that, with suitable protocols, the conformational sampling is hardly a bottleneck for computational modelling of Drug-like compounds.[46] Thus, the attention shifts to the more flexible compounds, many of which are relevant to drug discovery. With search parameters enhanced above default settings, several mainstream sampling methods yield robust and very encouraging results when working with larger and more flexible compounds.

Acknowledgments

Supplementary data

Supplementary data include the list of PDB entries and ligand codes for the bioactive X-ray structures of the compounds in the Drug-like, Flexible and Macrocycle sets. In addition, the 2D structures of the compounds (including hydrogens) associated with this article, and their X-ray coordinates, can be found, in the online version, at http://dx.doi.org/10.1016/j.bmc.2013.10.003.

References and notes

1. Brameld, K. A.; Kuhn, B.; Reuter, D. C.; Stahl, M. *J. Chem. Inf. Model.* **2008**, *48*, 1.
2. Chein, R. J.; Corey, E. J. *Org. Lett.* **2010**, *12*, 132.
3. Terhorst, J. P.; Jorgensen, W. L. *J. Chem. Theory Comput.* **2010**, *6*, 2762.
4. Taylor, R. *J. Chem. Inf. Model.* **2011**, *51*, 897.
5. Still, W. C.; Galynker, I. *Tetrahedron* **1981**, *37*, 3981.
6. Cruz-Cabeza, A. J.; Liebeschuetz, J. W.; Allen, F. H. *CrystEngComm* **2012**, *14*, 6797.
7. Wlodek, S.; Skillman, A. G.; Nicholls, A. *Acta Cryst.* **2006**, *D62*, 741.
8. Bell, J. A.; Ho, K. L.; Farid, R. *Acta Crystallogr., Sect. D* **2012**, *68*, 935.
9. Kolossvary, I.; Guida, W. C. *J. Am. Chem. Soc.* **1996**, *118*, 5011.
10. Matter, H.; Szilagyi, L.; Forgo, P.; Marinic, Z.; Klaic, B. *J. Am. Chem. Soc.* **1997**, *119*, 2212.
11. Lodewyk, M. W.; Siebert, M. R.; Tantillo, D. J. *Chem. Rev.* **2012**, *112*, 1839.
12. Blundell, C. D.; Packer, M. J.; Almond, A. *Bioorg. Med. Chem.* **2013**, *21*, 4976.
13. Jones, G.; Willett, P.; Glen, R. C. *J. Comput.-Aided Mol. Des.* **1995**, *9*, 532.
14. Labute, P.; Williams, C. *J. Med. Chem.* **2001**, *44*, 1483.
15. Leach, A. R.; Gillet, V. J.; Lewis, R. A.; Taylor, R. *J. Med. Chem.* **2010**, *53*, 539.
16. Foloppe, N.; Benwell, K.; Brooks, T. D.; Kennett, G.; Knight, A. R.; Misra, A.; Monck, N. J. T. *Bioorg. Med. Chem. Lett.* **2009**, *19*, 4183.
17. Nicholls, A.; McGaughey, G. B.; Sheridan, R. P.; Good, A. C.; Warren, G.; Mathieu, M.; Muchmore, S. W.; Brown, S. P.; Grant, J. A.; Haigh, J. A.; Nevins, N.; Jain, A. N.; Kelley, B. *J. Med. Chem.* **2010**, *53*, 3862.
18. Trott, O.; Olson, A. J. *J. Comput. Chem.* **2010**, *31*, 455.
19. Cheeseright, T.; Mackey, M.; Rose, S.; Vinter, A. *J. Chem. Inf. Model.* **2006**, *46*, 665.
20. Bostrom, J.; Norrby, P. O.; Liljefors, T. *J. Comput.-Aided Mol. Des.* **1998**, *12*, 383.
21. Perola, E.; Charifson, P. S. *J. Med. Chem.* **2004**, *47*, 2499.
22. Chen, I.; Foloppe, N. *J. Chem. Inf. Model.* **2008**, *48*, 1773.
23. Sitzmann, M.; Weidlich, I. E.; Filippov, I. V.; Liao, C.; Peach, M. L.; Ihlenfeldt, W.-D.; Karki, R. G.; Borodina, Y. V.; Cachau, R. E.; Nicklaus, M. C. *J. Chem. Inf. Model.* **2012**, *52*, 739.
24. Agrafiotis, D. K.; Gibbs, A. C.; Zhu, F.; Izrailev, S.; Martin, E. *J. Chem. Inf. Model.* **2007**, *47*, 1067.
25. Li, J.; Ehlers, T.; Sutter, J.; Varma-O'Brien, S.; Kirchmair, J. *J. Chem. Inf. Model.* **2007**, *47*, 1923.
26. Sperandio, O.; Souaille, M.; Delfaud, F.; Miteva, M. A.; Villoutreix, B. O. *Eur. J. Med. Chem.* **2009**, *44*, 1405.
27. Bonnet, P.; Agrafiotis, D. K.; Zhu, F.; Martin, E. *J. Chem. Inf. Model.* **2009**, *49*, 2242.
28. Liu, X.; Bai, F.; Ouyang, S.; Wang, X.; Li, H.; Jiang, H. *BMC Bioinformatics* **2009**, *10*, 101.
29. Watts, K. S.; Dalal, P.; Murphy, R. B.; Sherman, W.; Friesner, R. A.; Shelley, J. C. *J. Chem. Inf. Model.* **2010**, *50*, 534.
30. Chen, I.; Foloppe, N. *J. Chem. Inf. Model.* **2010**, *50*, 822.
31. Hawkins, P. C. D.; Skillman, A. G.; Warren, G. L.; Ellingson, B. A.; Stahl, M. T. *J. Chem. Inf. Model.* **2010**, *50*, 572.
32. Andronico, A.; Randall, A.; Benz, R. W.; Baldi, P. *J. Chem. Inf. Model.* **2011**, *51*, 760.
33. Bai, F.; Liu, X.; Li, J.; Zhang, H.; Jiang, H.; Wang, X.; Li, H. *BMC Bioinformatics* **2010**, *11*, 545.
34. Labute, P. *J. Chem. Inf. Model.* **2010**, *50*, 792.
35. Ebejer, J. P.; Morris, G. M.; Deane, C. *J. Chem. Inf. Model.* **2012**, *52*, 1146.
36. Hawkins, P. C. D.; Nicholls, A. *J. Chem. Inf. Model.* **2012**, *52*, 2919.
37. Schärfer, C.; Schulz-Gasch, T.; Ehrlich, H. C.; Guba, W.; Rarey, M.; Stahl, M. *J. Med. Chem.* **2013**, *56*, 2016.
38. Foloppe, N.; Chen, I. *Curr. Med. Chem.* **2009**, *16*, 3381.
39. Shim, J.; Mackerell, A. D. J. *MedChemComm* **2011**, *2*, 356.
40. Chang, G.; Guida, W. C.; Still, W. C. *J. Am. Chem. Soc.* **1989**, *111*, 4379.
41. Ferguson, D. M.; Raber, D. J. *J. Am. Chem. Soc.* **1989**, *111*, 4371.
42. Foloppe, N.; Nilsson, L. *J. Phys. Chem. B* **2005**, *109*, 9119.
43. Kolossvary, I.; Keseru, G. M. *J. Comput. Chem.* **2001**, *22*, 21.
44. Smellie, A.; Teig, S. L.; Towbin, P. *J. Comput. Chem.* **1995**, *16*, 171.
45. Izrailev, S.; Zhu, F.; Agrafiotis, D. K. *J. Comput. Chem.* **2006**, *27*, 1962.
46. Chen, I.; Foloppe, N. *Drug Dev. Res.* **2011**, *72*, 85.
47. Ledford, H. *Nature* **2010**, *468*, 608.
48. Mayer, A. M. S.; Glaser, K. B.; Cuevas, C.; Jacobs, R. S.; Kem, W.; Little, R. D.; McIntosh, J. M.; Newman, D. J.; Potts, B. C.; Shuster, D. E. *Trends Pharmacol. Sci.* **2010**, *31*, 255.
49. Foloppe, N.; Matassova, N.; Aboul-ela, F. *Drug Discovery Today* **2006**, *11*, 1019.
50. Vlieghe, P.; Lisowski, V.; Martinez, J.; Khrestchatisky, M. *Drug Discov. Today* **2010**, *15*, 40.
51. Driggers, E. M.; Hale, S. P.; Lee, J.; Terrett, N. K. *Nat. Rev. Drug Disc.* **2008**, *7*, 608.
52. Wells, J. A.; McClendon, C. L. *Nature* **2007**, *450*, 1001.
53. Diller, D. J.; Merz, K. M. *J. Comput.-Aided Mol. Des.* **2002**, *16*, 105.
54. Kolossvary, I.; Guida, W. C. *J. Comput. Chem.* **1999**, *20*, 1671.
55. Parish, C.; Lombardi, R.; Sinclair, K.; Smith, E.; Goldberg, A.; Rappleye, M.; Dure, M. *J. Mol. Graphics Modell.* **2002**, *21*, 129.
56. http://www.chemcomp.com/.
57. Mohamadi, F.; Richards, M. G. J.; Guida, W. C.; Liskamp, R.; Lipton, M.; Caufield, C.; Chang, G.; Hendrickson, T.; Still, W. C. *J. Comp. Chem.* **1990**, *11*, 440.
58. http://www.schrodinger.com.
59. Bostrom, J. *J. Comput.-Aided Mol. Design* **2001**, *15*, 1137.
60. Loferer, M. J.; Kolossvary, I.; Aszodi, A. *J. Mol. Graphics Modell.* **2007**, *25*, 700.
61. Halgren, T. *J. Comput. Chem.* **1996**, *17*, 490.
62. Jorgensen, W. L.; Maxwell, D. S.; Tirado-Rives, J. *J. Am. Chem. Soc.* **1996**, *118*, 11225.
63. Shivakumar, D.; Harder, E.; Damm, W.; Friesner, R. A.; Sherman, W. *J. Chem. Theory Comput.* **2012**, *8*, 2553.
64. Berman, H. M.; Westbrook, J.; Feng, Z.; Gilliland, G.; Bhat, T. N.; Weissig, H.; Shindyalov, I. N.; Bourne, P. E. *Nucleic Acids Res.* **2000**, *28*, 235.
65. Oprea, T. I. *J. Comput.-Aided Mol. Des.* **2000**, *14*, 251.
66. Onufriev, A.; Bashford, D.; Case, D. A. *J. Phys. Chem. B* **2000**, *104*, 3712.
67. Smellie, A.; Kahn, S. D.; Teig, S. L. *J. Chem. Inf. Comput. Sci.* **1995**, *35*, 285.
68. Borodina, Y.; Bolton, E.; Fontaine, F.; Bryant, S. H. *J. Chem. Inf. Model.* **2007**, *47*, 1428.
69. Saunders, M. *J. Am. Chem. Soc.* **1987**, *109*, 3150.
70. Nicklaus, M. C.; Shaomeng, W.; Driscoll, J. S.; Milne, W. A. *Biorg. Med. Chem.* **1995**, *3*, 411.
71. Kirchmair, J.; Laggner, C.; Wolber, G.; Langer, T. *J. Chem. Inf. Model.* **2005**, *45*, 422.
72. Ming-Hong, H.; Haq, O.; Muegge, I. *J. Chem. Inf. Model.* **2007**, *47*, 2242.